https://doi.org/10.1016/j.jsv.2021.116101

To: Journal of Sound and Vibration

Kron's substructuring method to the calculation of structural responses and response sensitivities of nonlinear systems

Wei Tian
PhD Student,
Department of Civil & Environmental Engineering,
The Hong Kong Polytechnic University,
Hung Hom, Kowloon, Hong Kong
cewei.tian@connect.polyu.hk

Shun Weng
Professor,
School of Civil and Hydraulic Engineering,
Huazhong University of Science and Technology,
Wuhan, Hubei, P. R. China
wengshun@hust.edu.cn

Yong Xia*
Professor,
Department of Civil & Environmental Engineering,
The Hong Kong Polytechnic University,
Hung Hom, Kowloon, Hong Kong
Tel: (852) 27666066
ceyxia@polyu.edu.hk

* Corresponding author

Abstract

Numerous civil engineering structures exhibit nonlinearities. Even though the nonlinearities constitute only a small part of the structure, the entire structure behaves nonlinearly, and the analysis of the whole structure is consequently computationally expensive. This paper develops ~~the~~ Kron's substructuring method for fast computation of the structural responses and response sensitivities of nonlinear systems. The nonlinearity is detected and located using the ordinary coherence function. The global structure is then divided into linear and nonlinear substructures. The local nonlinearities are thus restricted in a few nonlinear substructures. The linear substructural responses are interpreted as the combination of a few master modal responses based on the mode superposition. The discarded slave modal responses of the linear substructures are compensated by the corresponding master modal responses, nonlinear substructural responses and external excitation on the linear substructures with their associated transformation matrices. A reduced vibration equation of a much smaller size is derived with the transformation matrices. The structural responses and response sensitivities are then calculated from the reduced vibration equation. The precision and efficiency of the proposed method are finally verified by a nonlinear spring-mass system and a relatively large-scale nonlinear frame.

Keywords: substructuring method; nonlinear systems; sensitivity analysis; Kron's method

1. Introduction

Most practical engineering structures are nonlinear to some extent due to one or a combination of several factors [1, 2]. For instance, a reinforced concrete structure in the presence of cracks exhibits nonlinearities. The boundary conditions, looseness of some joints and nonlinear components such as shock absorbers, vibration isolators, bearings or dampers, also cause nonlinearities to the structure. Though the nonlinearities usually occur in a few local regions only, the whole structure behaves nonlinearly.

Calculation of structural responses and response sensitivities is significant in civil engineering for various applications such as system identification, damage detection, reliability analysis, structural design optimization and so on [3-7]. The structural responses of nonlinear systems are usually calculated using the numerical integration methods, like Newmark-β method, Wilson-θ method, etc., with an iterative process embedded in each time step to determine the time-variant system matrices [8]. The response sensitivities are computed in terms of the derivatives of the structural responses with respect to the design parameters with various techniques, including the finite difference method [9], perturbation method [10], adjoint structure method [11] and direct differentiation method [12]. These methods compute the structural responses and response sensitivities in the global structure level with numerous iterations, which is very computationally expensive when a large nonlinear structure with numerous time steps is concerned.

Substructuring methods are efficient to deal with large-size problems [13, 14]. The methods partition the global structure rationally into several substructures to be analyzed independently. A reduced model is constructed with the substructural solutions to recover the global dynamic properties. As the global structure is divided into smaller substructures, it is easier and quicker to analyze the substructural system matrices. Besides, the substructuring methods allow for the concerned substructures to be analyzed independently, which enables parallel computation. Hurty [15] first proposed the substructuring method with a fixed-interface condition.; Tthis method was later popularized by Craig and Bampton [16] to calculate the lower modes of large-scale structures. Qu [17] employed the dynamic condensation technique in the substructure level to reduce the size of the finite element model of large structures with local nonlinearities. Apiwattanalunggarn et al. [18] firstly developed the Craig-Bampton method to compute the free-vibration responses of nonlinear systems using nonlinear normal mode (NNM). The method was limited to weakly nonlinear systems and it generated the substructural reduced--order models with only one NNM invariant manifold, which is computationally demanding for a large nonlinear structure requiring the multi-NNM invariant manifold [19, 20]. Kerschen et al. [21] employed the Craig-Bampton method to condense the linear substructures to improve the computational efficiency of NNMs of a full-scale aircraft. Joannin et al. [22] extended the Craig-Bampton method to strongly nonlinear systems using the nonlinear complex modes.

Fang et al. [23] proposed an adaptive modified Craig-Bampton method to solve the structural dynamic response for nonlinear tall buildings with high efficiency. Latini and Brunetti [24] employed the substructuring methods and NNM to analyze the dynamic behavior of complex systems with nonlinear connections.

Kron [25] proposed a substructuring method with free-interface condition for electrical problems, which was then modified for dynamic analysis of large structures via a receptance matrix by Simpson and Tabarrok [26]. Simpson [27] later developed the Kron's method to calculate the eigenvalue and vector sensitivities using an intersection matrix of small order. Kron's substructuring method has some distinctive advantages over the Craig-Bampton method in dealing with large-scale structures. It assembles the substructures in a dual form with free-interface condition. Due to this, the size of the reduced model is irrelevant to the numerous interface degrees of freedom (DOFs) of a large structure [13, 14]. The Kron's substructuring method is also superior to cope with the complicated interface cases when some interface DOFs are shared by three or more substructures. Recently, the Kron's method has been developed for dynamic responses, sensitivity analysis, model updating and damage detection of large-scale linear structures [28-34].

In the existing substructuring methods, the structural responses are usually expressed in modal responses through mode superposition. A reduced vibration equation is derived with only some lowest modes (master modes) retained in each substructure while ~~the~~ higher modes (slave modes) are discarded directly or compensated by the residual flexibility [28, 29] or an iterative scheme [30, 31]. These substructuring methods apply to linear systems only due to the inapplicability of the mode superposition to nonlinear systems.

This paper develops the Kron's substructuring method to compute the structural responses and response sensitivities of nonlinear systems. The presence and location of nonlinearity is detected using the ordinary coherence function. The global structure is then divided into nonlinear and linear substructures. After division, the nonlinearities are restricted in a few specific nonlinear substructures. The linear substructures are treated as the independent linear structures. The mode superposition is used to interpret the linear substructural responses as the combination of a few master modal responses. The discarded slave modal responses of the linear substructures are compensated by the corresponding master modal responses, nonlinear substructural responses and external excitation on the linear substructures with their associated transformation matrices. A reduced vibration equation is constructed with the transformation matrices, and the size of the reduced vibration equation is significantly smaller than that of the original global structure. Since the linear substructures are ~~largely~~ reduced significantly and the nonlinear substructure is localized, the structural responses and response sensitivities are computed efficiently from the reduced vibration equation.

2. Substructuring method for structural responses of nonlinear systems

The vibration equation of a nonlinear system of n DOFs is expressed as

$$\mathbf{M}\ddot{\mathbf{x}}(t)+\mathbf{C}(\mathbf{x})\dot{\mathbf{x}}(t)+\mathbf{K}(\mathbf{x})\mathbf{x}(t)=\mathbf{f}(t) \tag{1}$$

where $\ddot{\mathbf{x}}(t)$, $\dot{\mathbf{x}}(t)$ and $\mathbf{x}(t)$ are respectively the acceleration, velocity and displacement vectors of the structure at time step t; $\mathbf{f}(t)$ is the external force imposed on the system; $\mathbf{M}$ is the system mass matrix, which is treated as a constant for the nonlinear system; $\mathbf{C}(\mathbf{x})$ and $\mathbf{K}(\mathbf{x})$, being the nonlinear functions of $\mathbf{x}$, are the time-variant damping and stiffness matrices of the nonlinear system, respectively. If the Rayleigh damping is assumed, $\mathbf{C}(\mathbf{x})=a_1\mathbf{M}+a_2\mathbf{K}(\mathbf{x})$, where a_1 and a_2 are respectively the damping coefficients associated with the mass and stiffness matrices. For brevity, time variable t is omitted hereinafter.

In practical nonlinear systems, the nonlinearities usually exist in a few local areas, the nonlinear system can thus be divided into linear and nonlinear substructures. Assume the global nonlinear system is divided into NS substructures. The 1^{st}-NL^{th} substructures are the linear substructures and the $(NL+1)^{th}$-NS^{th} substructures are the nonlinear substructures. The vibration equation of the j^{th} linear substructure is expressed as

$$\mathbf{M}^{(j)}\ddot{\mathbf{x}}^{(j)}+\mathbf{C}^{(j)}\dot{\mathbf{x}}^{(j)}+\mathbf{K}^{(j)}\mathbf{x}^{(j)}=\mathbf{f}^{(j)}+\mathbf{g}^{(j)} \tag{2}$$

where $\mathbf{g}$ are the substructural connection forces in the interface DOFs, superscript (j) denotes the variables associated with the j^{th} linear substructure (j=1, 2, …, NL). The vibration equation of the k^{th} nonlinear substructure is expressed as

$$\mathbf{M}^{(k)}\ddot{\mathbf{x}}^{(k)}+\mathbf{C}^{(k)}\left(\mathbf{x}^{(k)}\right)\dot{\mathbf{x}}^{(k)}+\mathbf{K}^{(k)}\left(\mathbf{x}^{(k)}\right)\mathbf{x}^{(k)}=\mathbf{f}^{(k)}+\mathbf{g}^{(k)} \tag{3}$$

where superscript (k) represents the variables related to the k^{th} nonlinear substructure (k=NL+1, NL+2, …, NS). It is noted that after division, only the damping and stiffness matrices of the nonlinear substructures are time-variant, that is, the local nonlinearities are restricted within a few nonlinear substructures.

The system matrices of the linear and nonlinear substructures are assembled respectively as

$$\mathbf{M}^{L} = diag\left(\mathbf{M}^{(1)},\cdots,\mathbf{M}^{(NL)}\right),\ \ \mathbf{M}^{N} = diag\left(\mathbf{M}^{(NL+1)},\cdots,\mathbf{M}^{(NS)}\right) \tag{4}$$

$$\mathbf{C}^{L} = diag\left(\mathbf{C}^{(1)},\cdots,\mathbf{C}^{(NL)}\right),\ \ \mathbf{C}^{N}\left(\mathbf{x}^{N}\right) = diag\left(\mathbf{C}^{(NL+1)}\left(\mathbf{x}^{(NL+1)}\right),\cdots,\mathbf{C}^{(NS)}\left(\mathbf{x}^{(NS)}\right)\right) \tag{5}$$

$$\mathbf{K}^{L} = diag\left(\mathbf{K}^{(1)},\cdots,\mathbf{K}^{(NL)}\right),\ \ \mathbf{K}^{N}\left(\mathbf{x}^{N}\right) = diag\left(\mathbf{K}^{(NL+1)}\left(\mathbf{x}^{(NL+1)}\right),\cdots,\mathbf{K}^{(NS)}\left(\mathbf{x}^{(NS)}\right)\right) \tag{6}$$

$$\ddot{\mathbf{x}}^{L} = \begin{Bmatrix} \ddot{\mathbf{x}}^{(1)} \\ \vdots \\ \ddot{\mathbf{x}}^{(NL)} \end{Bmatrix}, \dot{\mathbf{x}}^{L} = \begin{Bmatrix} \dot{\mathbf{x}}^{(1)} \\ \vdots \\ \dot{\mathbf{x}}^{(NL)} \end{Bmatrix}, \mathbf{x}^{L} = \begin{Bmatrix} \mathbf{x}^{(1)} \\ \vdots \\ \mathbf{x}^{(NL)} \end{Bmatrix}, \ddot{\mathbf{x}}^{N} = \begin{Bmatrix} \ddot{\mathbf{x}}^{(NL+1)} \\ \vdots \\ \ddot{\mathbf{x}}^{(NS)} \end{Bmatrix}, \dot{\mathbf{x}}^{N} = \begin{Bmatrix} \dot{\mathbf{x}}^{(NL+1)} \\ \vdots \\ \dot{\mathbf{x}}^{(NS)} \end{Bmatrix}, \mathbf{x}^{N} = \begin{Bmatrix} \mathbf{x}^{(NL+1)} \\ \vdots \\ \mathbf{x}^{(NS)} \end{Bmatrix} \tag{7}$$

$$\mathbf{f}^{L} = \begin{Bmatrix} \mathbf{f}^{(1)} \\ \vdots \\ \mathbf{f}^{(NL)} \end{Bmatrix}, \mathbf{f}^{N} = \begin{Bmatrix} \mathbf{f}^{(NL+1)} \\ \vdots \\ \mathbf{f}^{(NS)} \end{Bmatrix} \tag{8}$$

$$\mathbf{g}^{L} = \begin{Bmatrix} \mathbf{g}^{(1)} \\ \vdots \\ \mathbf{g}^{(NL)} \end{Bmatrix}, \mathbf{g}^{N} = \begin{Bmatrix} \mathbf{g}^{(NL+1)} \\ \vdots \\ \mathbf{g}^{(NS)} \end{Bmatrix} \tag{9}$$

where superscripts L and N respectively denote the assembled vectors or matrices from the linear and nonlinear substructures; and *diag* represents the diagonal assembly of variables. For brevity, the time-variant system matrices $\mathbf{C}^{N}\left(\mathbf{x}^{N}\right)$ and $\mathbf{K}^{N}\left(\mathbf{x}^{N}\right)$ are simplified as $\mathbf{C}^{N}$ and $\mathbf{K}^{N}$.

The vibration equations of the linear and nonlinear substructures are assembled as

$$\mathbf{M}^L\ddot{\mathbf{x}}^L + \mathbf{C}^L\dot{\mathbf{x}}^L + \mathbf{K}^L\mathbf{x}^L = \mathbf{f}^L + \mathbf{g}^L \tag{10}$$

$$\mathbf{M}^N\ddot{\mathbf{x}}^N + \mathbf{C}^N\dot{\mathbf{x}}^N + \mathbf{K}^N\mathbf{x}^N = \mathbf{f}^N + \mathbf{g}^N \tag{11}$$

The substructures satisfy the displacement compatibility and force equilibrium conditions in the interface as [13, 14]

$$\mathbf{D}\bar{\mathbf{x}} = \begin{bmatrix}\mathbf{D}^L & \mathbf{D}^N\end{bmatrix}\begin{Bmatrix}\mathbf{x}^L \\ \mathbf{x}^N\end{Bmatrix} = \mathbf{D}^L\mathbf{x}^L + \mathbf{D}^N\mathbf{x}^N = \mathbf{0} \tag{12}$$

$$\bar{\mathbf{g}} = \mathbf{D}^T\boldsymbol{\tau} = \begin{bmatrix}\mathbf{g}^L & \mathbf{g}^N\end{bmatrix} = \begin{bmatrix}\left[\mathbf{D}^L\right]^T\boldsymbol{\tau} & \left[\mathbf{D}^N\right]^T\boldsymbol{\tau}\end{bmatrix} \tag{13}$$

where $\mathbf{D} = \begin{bmatrix}\mathbf{D}^L & \mathbf{D}^N\end{bmatrix}$ is a signed Boolean matrix to indicate the connection relationship between adjacent substructures~~, for example, 1 and -1 for a rigid connection~~; $\mathbf{D}^L$ and $\mathbf{D}^N$ are respectively the corresponding component matrices associated with the linear and nonlinear substructural DOFs;~~.~~ $\bar{\mathbf{x}} = \begin{Bmatrix}\mathbf{x}^L & \mathbf{x}^N\end{Bmatrix}^T$ is the assembled displacement vector of the linear and nonlinear substructures; $\bar{\mathbf{g}} = \begin{bmatrix}\mathbf{g}^L & \mathbf{g}^N\end{bmatrix}$ encloses the interface connection forces of the linear and nonlinear substructures; $\boldsymbol{\tau}$ ~~are~~ is the Lagrange multiplier~~s~~, which impl<u>ies</u>~~y~~ the interface intensities; and superscript T denotes the transpose of a matrix.

Eqs. (10)-(13) are the primal formulation of the substructural vibration equation, which can be rewritten in a dual form as

$$\begin{bmatrix}\mathbf{M}^L & \mathbf{0} & \mathbf{0} \\ \mathbf{0} & \mathbf{M}^N & \mathbf{0} \\ \mathbf{0} & \mathbf{0} & \mathbf{0}\end{bmatrix}\begin{Bmatrix}\ddot{\mathbf{x}}^L \\ \ddot{\mathbf{x}}^N \\ \ddot{\boldsymbol{\tau}}\end{Bmatrix} + \begin{bmatrix}\mathbf{C}^L & \mathbf{0} & \mathbf{0} \\ \mathbf{0} & \mathbf{C}^N & \mathbf{0} \\ \mathbf{0} & \mathbf{0} & \mathbf{0}\end{bmatrix}\begin{Bmatrix}\dot{\mathbf{x}}^L \\ \dot{\mathbf{x}}^N \\ \dot{\boldsymbol{\tau}}\end{Bmatrix} + \begin{bmatrix}\mathbf{K}^L & \mathbf{0} & -\left[\mathbf{D}^L\right]^T \\ \mathbf{0} & \mathbf{K}^N & -\left[\mathbf{D}^N\right]^T \\ -\mathbf{D}^L & -\mathbf{D}^N & \mathbf{0}\end{bmatrix}\begin{Bmatrix}\mathbf{x}^L \\ \mathbf{x}^N \\ \boldsymbol{\tau}\end{Bmatrix} = \begin{Bmatrix}\mathbf{f}^L \\ \mathbf{f}^N \\ \mathbf{0}\end{Bmatrix} \tag{14}$$

The linear substructures are treated as independent linear structures, whose dynamic responses can be expressed by the mode superposition as

$$\mathbf{x}^L = \mathbf{\Phi}^L \mathbf{z}^L ,\ \ \dot{\mathbf{x}}^L = \mathbf{\Phi}^L \dot{\mathbf{z}}^L ,\ \ \ddot{\mathbf{x}}^L = \mathbf{\Phi}^L \ddot{\mathbf{z}}^L \tag{15}$$

where $\mathbf{z}^L$, $\dot{\mathbf{z}}^L$ and $\ddot{\mathbf{z}}^L$ are respectively the coordinates of $\mathbf{x}^L$, $\dot{\mathbf{x}}^L$ and $\ddot{\mathbf{x}}^L$ in modal space $\mathbf{\Phi}^L$. $\mathbf{\Phi}^L$ is the eigenvector of the assembled linear substructures, which is expressed as

$$\mathbf{\Phi}^L = diag\left(\mathbf{\Phi}^{(1)} \quad \cdots \quad \mathbf{\Phi}^{(j)} \quad \cdots \quad \mathbf{\Phi}^{(NL)}\right) \tag{16}$$

$\mathbf{\Phi}^{(j)}$ is calculated from the eigenequation of the j^{th} linear substructure by

$$\mathbf{K}^{(j)}\mathbf{\Phi}^{(j)} = \mathbf{\Lambda}^{(j)}\mathbf{M}^{(j)}\mathbf{\Phi}^{(j)} \tag{17}$$

where $\mathbf{\Lambda}^{(j)}$ and $\mathbf{\Phi}^{(j)}$ are the eigenvalue and eigenvector matrices of the j^{th} linear substructure, respectively. $\mathbf{\Lambda}^{(j)}$ and $\mathbf{\Phi}^{(j)}$ satisfy the orthogonal conditions of

$$\left[\mathbf{\Phi}^{(j)}\right]^T \mathbf{M}^{(j)}\mathbf{\Phi}^{(j)} = \mathbf{I} \tag{18}$$

$$\left[\mathbf{\Phi}^{(j)}\right]^T \mathbf{K}^{(j)}\mathbf{\Phi}^{(j)} = \mathbf{\Lambda}^{(j)} \tag{19}$$

Accordingly, the assembled eigen-matrices also satisfy the orthogonal conditions of

$$\left[\mathbf{\Phi}^{L}\right]^T \mathbf{M}^{L}\mathbf{\Phi}^{L} = \mathbf{I}^L \tag{20}$$

$$\left[\mathbf{\Phi}^{L}\right]^T \mathbf{K}^{L}\mathbf{\Phi}^{L} = \mathbf{\Lambda}^L \tag{21}$$

$$\left[\mathbf{\Phi}^{L}\right]^T \mathbf{C}^{L}\mathbf{\Phi}^{L} = \left[\mathbf{\Phi}^{L}\right]^T \left(a_1\mathbf{M}^L + a_2\mathbf{K}^L\right)\mathbf{\Phi}^{L} = a_1\mathbf{I}^L + a_2\mathbf{\Lambda}^L \tag{22}$$

$\mathbf{\Lambda}^L = diag\left(\mathbf{\Lambda}^{(1)} \quad \cdots \quad \mathbf{\Lambda}^{(j)} \quad \cdots \quad \mathbf{\Lambda}^{(NL)}\right)$ are the diagonally assembled eigenvalues of all linear substructures.

Pre-multiplying the first line of Eq. (14) with $\left[\mathbf{\Phi}^{L}\right]^T$ and considering Eq. (15) and the orthogonal conditions in Eqs. (20)-(22), Eq. (14) is rewritten as

$$\begin{bmatrix} \mathbf{I}^L & \mathbf{0} & \mathbf{0} \\ \mathbf{0} & \mathbf{M}^N & \mathbf{0} \\ \mathbf{0} & \mathbf{0} & \mathbf{0} \end{bmatrix} \begin{Bmatrix} \ddot{\mathbf{z}}^L \\ \ddot{\mathbf{x}}^N \\ \ddot{\boldsymbol{\tau}} \end{Bmatrix} + \begin{bmatrix} a_1\mathbf{I}^L + a_2\boldsymbol{\Lambda}^L & \mathbf{0} & \mathbf{0} \\ \mathbf{0} & \mathbf{C}^N & \mathbf{0} \\ \mathbf{0} & \mathbf{0} & \mathbf{0} \end{bmatrix} \begin{Bmatrix} \dot{\mathbf{z}}^L \\ \dot{\mathbf{x}}^N \\ \dot{\boldsymbol{\tau}} \end{Bmatrix} + \begin{bmatrix} \boldsymbol{\Lambda}^L & \mathbf{0} & -\left[\mathbf{D}^L\boldsymbol{\Phi}^L\right]^T \\ \mathbf{0} & \mathbf{K}^N & -\left[\mathbf{D}^N\right]^T \\ -\mathbf{D}^L\boldsymbol{\Phi}^L & -\mathbf{D}^N & \mathbf{0} \end{bmatrix} \begin{Bmatrix} \mathbf{z}^L \\ \mathbf{x}^N \\ \boldsymbol{\tau} \end{Bmatrix}$$
$$= \begin{Bmatrix} \left[\boldsymbol{\Phi}^L\right]^T \mathbf{f}^L \\ \mathbf{f}^N \\ \mathbf{0} \end{Bmatrix} \tag{23}$$

Eq. (23) includes the substructural interface DOFs. It has a larger size than the original global vibration equation Eq. (1) and thus is inefficient to be solved directly. As a solution, a reduced vibration equation of much smaller size is derived. For brevity, this paper only derives the formulas of the undamped nonlinear systems. The case with Rayleigh damping can be derived similarly and will be given directly later. The undamped case of the vibration equation (Eq. (23)) is expressed as

$$\begin{bmatrix} \mathbf{I}^L & \mathbf{0} & \mathbf{0} \\ \mathbf{0} & \mathbf{M}^N & \mathbf{0} \\ \mathbf{0} & \mathbf{0} & \mathbf{0} \end{bmatrix} \begin{Bmatrix} \ddot{\mathbf{z}}^L \\ \ddot{\mathbf{x}}^N \\ \ddot{\boldsymbol{\tau}} \end{Bmatrix} + \begin{bmatrix} \boldsymbol{\Lambda}^L & \mathbf{0} & -\left[\mathbf{D}^L\boldsymbol{\Phi}^L\right]^T \\ \mathbf{0} & \mathbf{K}^N & -\left[\mathbf{D}^N\right]^T \\ -\mathbf{D}^L\boldsymbol{\Phi}^L & -\mathbf{D}^N & \mathbf{0} \end{bmatrix} \begin{Bmatrix} \mathbf{z}^L \\ \mathbf{x}^N \\ \boldsymbol{\tau} \end{Bmatrix} = \begin{Bmatrix} \left[\boldsymbol{\Phi}^L\right]^T \mathbf{f}^L \\ \mathbf{f}^N \\ \mathbf{0} \end{Bmatrix} \tag{24}$$

The complete eigenmodes of each linear substructure are divided into master and slave modes. Eq. (24) is thus rewritten as

$$\begin{bmatrix} \mathbf{I}_m^L & \mathbf{0} & \mathbf{0} & \mathbf{0} \\ \mathbf{0} & \mathbf{I}_s^L & \mathbf{0} & \mathbf{0} \\ \mathbf{0} & \mathbf{0} & \mathbf{M}^N & \mathbf{0} \\ \mathbf{0} & \mathbf{0} & \mathbf{0} & \mathbf{0} \end{bmatrix} \begin{Bmatrix} \ddot{\mathbf{z}}_m^L \\ \ddot{\mathbf{z}}_s^L \\ \ddot{\mathbf{x}}^N \\ \ddot{\boldsymbol{\tau}} \end{Bmatrix} + \begin{bmatrix} \boldsymbol{\Lambda}_m^L & \mathbf{0} & \mathbf{0} & -\left[\mathbf{D}^L\boldsymbol{\Phi}_m^L\right]^T \\ \mathbf{0} & \boldsymbol{\Lambda}_s^L & \mathbf{0} & -\left[\mathbf{D}^L\boldsymbol{\Phi}_s^L\right]^T \\ \mathbf{0} & \mathbf{0} & \mathbf{K}^N & -\left[\mathbf{D}^N\right]^T \\ -\mathbf{D}^L\boldsymbol{\Phi}_m^L & -\mathbf{D}^L\boldsymbol{\Phi}_s^L & -\mathbf{D}^N & \mathbf{0} \end{bmatrix} \begin{Bmatrix} \mathbf{z}_m^L \\ \mathbf{z}_s^L \\ \mathbf{x}^N \\ \boldsymbol{\tau} \end{Bmatrix} = \begin{Bmatrix} \left[\boldsymbol{\Phi}_m^L\right]^T \mathbf{f}^L \\ \left[\boldsymbol{\Phi}_s^L\right]^T \mathbf{f}^L \\ \mathbf{f}^N \\ \mathbf{0} \end{Bmatrix}$$

(25)

where subscripts *m* and *s* denote the system variables associated with the master and slave modes of the linear substructures, respectively. $\mathbf{\Lambda}_m^L$, $\mathbf{\Lambda}_s^L$, $\mathbf{\Phi}_m^L$ and $\mathbf{\Phi}_s^L$ are assembled from the substructural master modes, and take the form of

$$\mathbf{\Lambda}_m^L = diag\left(\mathbf{\Lambda}_m^{(1)} \quad \cdots \quad \mathbf{\Lambda}_m^{(j)} \quad \cdots \quad \mathbf{\Lambda}_m^{(NL)}\right), \mathbf{\Lambda}_m^{(j)} = diag\left(\lambda_1^{(j)} \quad \lambda_2^{(j)} \quad \cdots \quad \lambda_{m^{(j)}}^{(j)}\right) \tag{26}$$

$$\mathbf{\Lambda}_s^L = diag\left(\mathbf{\Lambda}_s^{(1)} \quad \cdots \quad \mathbf{\Lambda}_s^{(j)} \quad \cdots \quad \mathbf{\Lambda}_s^{(NL)}\right), \mathbf{\Lambda}_s^{(j)} = diag\left(\lambda_{m^{(j)}+1}^{(j)} \quad \lambda_{m^{(j)}+2}^{(j)} \quad \cdots \quad \lambda_{m^{(j)}+s^{(j)}}^{(j)}\right) \tag{27}$$

$$\mathbf{\Phi}_m^L = diag\left(\mathbf{\Phi}_m^{(1)} \quad \cdots \quad \mathbf{\Phi}_m^{(j)} \quad \cdots \quad \mathbf{\Phi}_m^{(NL)}\right), \mathbf{\Phi}_m^{(j)} = diag\left(\boldsymbol{\phi}_1^{(j)} \quad \boldsymbol{\phi}_2^{(j)} \quad \cdots \quad \boldsymbol{\phi}_{m^{(j)}}^{(j)}\right) \tag{28}$$

$$\mathbf{\Phi}_s^L = diag\left(\mathbf{\Phi}_s^{(1)} \quad \cdots \quad \mathbf{\Phi}_s^{(j)} \quad \cdots \quad \mathbf{\Phi}_s^{(NL)}\right), \mathbf{\Phi}_s^{(j)} = diag\left(\boldsymbol{\phi}_{m^{(j)}+1}^{(j)} \quad \boldsymbol{\phi}_{m^{(j)}+2}^{(j)} \quad \cdots \quad \boldsymbol{\phi}_{m^{(j)}+s^{(j)}}^{(j)}\right) \tag{29}$$

where λ and $\boldsymbol{\phi}$ are respectively the eigenvalue and eigenvector of a specific substructural mode; and $m^{(j)}$ and $s^{(j)}$ are respectively the number of master and slave modes of the j^{th} linear substructure.

The second line of Eq. (25) gives

$$\mathbf{z}_s^L = -\left(\mathbf{\Lambda}_s^L\right)^{-1} \ddot{\mathbf{z}}_s^L + \left(\mathbf{\Lambda}_s^L\right)^{-1} \left[\mathbf{D}^L \mathbf{\Phi}_s^L\right]^T \boldsymbol{\tau} + \left(\mathbf{\Lambda}_s^L\right)^{-1} \left[\mathbf{\Phi}_s^L\right]^T \mathbf{f}^L \tag{30}$$

Substituting Eq. (30) into the fourth line of Eq. (25) and considering the orthogonal condition of $\left[\mathbf{\Phi}_s^L\right]^T \mathbf{M}^L \mathbf{\Phi}_s^L = \mathbf{I}_s^L$, one can obtain

$$\boldsymbol{\tau} = \left(\mathbf{D}^L \mathbf{F}^L \left[\mathbf{D}^L\right]^T\right)^{-1} \left(\mathbf{D}^L \mathbf{F}^L \mathbf{M}^L \mathbf{\Phi}_s^L \ddot{\mathbf{z}}_s^L - \mathbf{D}^L \mathbf{\Phi}_m^L \mathbf{z}_m^L - \mathbf{D}^N \mathbf{x}^N - \mathbf{D}^L \mathbf{F}^L \mathbf{f}^L\right) \tag{31}$$

where $\mathbf{F}^L = \mathbf{\Phi}_s^L \left(\mathbf{\Lambda}_s^L\right)^{-1} \left[\mathbf{\Phi}_s^L\right]^T$ is the residual flexibility of the assembled linear substructures. It is calculated from the stiffness and master modes of each linear substructure by [28]

$$\mathbf{F}^L = diag\left(\left[\mathbf{K}^{(1)}\right]^{-1} - \mathbf{\Phi}_m^{(1)} \left[\mathbf{\Lambda}_m^{(1)}\right]^{-1} \left[\mathbf{\Phi}_m^{(1)}\right]^T \quad \cdots \quad \left[\mathbf{K}^{(NL)}\right]^{-1} - \mathbf{\Phi}_m^{(NL)} \left[\mathbf{\Lambda}_m^{(NL)}\right]^{-1} \left[\mathbf{\Phi}_m^{(NL)}\right]^T\right)$$

(32)

Pre-multiplying Eq. (30) with $\mathbf{\Phi}_s^L$ and considering Eq. (31), one can obtain

$$\begin{aligned}\mathbf{\Phi}_s^L\mathbf{z}_s^L &= \mathbf{F}^L\left[\mathbf{D}^L\right]^T\left(\mathbf{D}^L\mathbf{F}^L\left[\mathbf{D}^L\right]^T\right)^{-1}\left(\mathbf{D}^L\mathbf{F}^L\mathbf{M}^L\mathbf{\Phi}_s^L\ddot{\mathbf{z}}_s^L - \mathbf{D}^L\mathbf{\Phi}_m^L\mathbf{z}_m^L - \mathbf{D}^N\mathbf{x}^N - \mathbf{D}^L\mathbf{F}^L\mathbf{f}^L\right)\\ &\quad -\mathbf{F}^L\mathbf{M}^L\mathbf{\Phi}_s^L\ddot{\mathbf{z}}_s^L + \mathbf{F}^L\mathbf{f}^L\\ &= -\mathbf{T}^L\mathbf{z}_m^L - \mathbf{T}^N\mathbf{x}^N - \mathbf{S}\mathbf{M}^L\mathbf{\Phi}_s^L\ddot{\mathbf{z}}_s^L + \mathbf{S}\mathbf{f}^L\end{aligned} \tag{33}$$

where

$$\mathbf{T}^L = \mathbf{F}^L\left[\mathbf{D}^L\right]^T\left(\mathbf{D}^L\mathbf{F}^L\left[\mathbf{D}^L\right]^T\right)^{-1}\mathbf{D}^L\mathbf{\Phi}_m^L \tag{34}$$

$$\mathbf{T}^N = \mathbf{F}^L\left[\mathbf{D}^L\right]^T\left(\mathbf{D}^L\mathbf{F}^L\left[\mathbf{D}^L\right]^T\right)^{-1}\mathbf{D}^N \tag{35}$$

$$\mathbf{S} = \mathbf{F}^L - \mathbf{F}^L\left[\mathbf{D}^L\right]^T\left(\mathbf{D}^L\mathbf{F}^L\left[\mathbf{D}^L\right]^T\right)^{-1}\mathbf{D}^L\mathbf{F}^L \tag{36}$$

The item $\mathbf{S}\mathbf{M}^L\mathbf{\Phi}_s^L\ddot{\mathbf{z}}_s^L$ in Eq. (33) is associated with the slave modes. It has little contribution to structural vibration in terms of energy and is thus neglected [14, 34], which will be verified in the numerical example in Section 4. Eq. (33) is therefore simplified into

$$\mathbf{\Phi}_s^L\mathbf{z}_s^L = -\mathbf{T}^L\mathbf{z}_m^L - \mathbf{T}^N\mathbf{x}^N + \mathbf{S}\mathbf{f}^L \tag{37}$$

Accordingly, one can obtain

$$\mathbf{\Phi}_s^L\ddot{\mathbf{z}}_s^L = -\mathbf{T}^L\ddot{\mathbf{z}}_m^L - \mathbf{T}^N\ddot{\mathbf{x}}^N + \mathbf{S}\ddot{\mathbf{f}}^L \tag{38}$$

where $\ddot{\mathbf{f}}^L$ is the second-order derivative of $\mathbf{f}^L$ with respect to time *t*. For a practical structure, $\ddot{\mathbf{f}}^L$ can be calculated with the finite difference method or derived directly if $\mathbf{f}^L$ is an explicit function of *t*. Eqs. (37) and (38) show that the structural responses contributed by the slave modes $\mathbf{\Phi}_s^L\mathbf{z}_s^L$ can be transformed to those by the master modal responses of the linear substructures $\mathbf{z}_m^L$, responses of the nonlinear substructures $\mathbf{x}^N$

and external excitation at the linear substructures $\mathbf{f}^L$. $\mathbf{T}^L$, $\mathbf{T}^N$ and $\mathbf{S}$ act as the corresponding transformation matrices.

Substituting Eqs. (31) and (38) into the first and third lines of Eq. (25) and considering $\mathbf{F}^L\mathbf{K}^L\mathbf{F}^L = \mathbf{F}^L$ [32], one can obtain

$$\begin{bmatrix} \mathbf{I}^L + \left[\mathbf{T}^L\right]^T \mathbf{M}^L\mathbf{T}^L & \left[\mathbf{T}^L\right]^T \mathbf{M}^L\mathbf{T}^N \\ \left[\mathbf{T}^N\right]^T \mathbf{M}^L\mathbf{T}^L & \mathbf{M}^N + \left[\mathbf{T}^N\right]^T \mathbf{M}^L\mathbf{T}^N \end{bmatrix} \begin{Bmatrix} \ddot{\mathbf{z}}_m^L \\ \ddot{\mathbf{x}}^N \end{Bmatrix} + \begin{bmatrix} \mathbf{\Lambda}_m^L + \left[\mathbf{T}^L\right]^T \mathbf{K}^L\mathbf{T}^L & \left[\mathbf{T}^L\right]^T \mathbf{K}^L\mathbf{T}^N \\ \left[\mathbf{T}^N\right]^T \mathbf{K}^L\mathbf{T}^L & \mathbf{K}^N + \left[\mathbf{T}^N\right]^T \mathbf{K}^L\mathbf{T}^N \end{bmatrix} \begin{Bmatrix} \mathbf{z}_m^L \\ \mathbf{x}^N \end{Bmatrix}$$
$$= \begin{Bmatrix} \left(\mathbf{\Phi}_m^L - \mathbf{T}^L\right)^T \mathbf{f}^L + \left[\mathbf{T}^L\right]^T \mathbf{M}^L\mathbf{S}\ddot{\mathbf{f}}^L \\ \mathbf{f}^N - \left[\mathbf{T}^N\right]^T \mathbf{f}^L + \left[\mathbf{T}^N\right]^T \mathbf{M}^L\mathbf{S}\ddot{\mathbf{f}}^L \end{Bmatrix} \tag{39}$$

Eq. (39) is the reduced vibration equation of the undamped nonlinear system in terms of $\mathbf{z}_m^L$ and $\mathbf{x}^N$. The Rayleigh damping is linearly associated with the structural mass and stiffness matrix, and the reduced vibration equation for the damped case can thus be derived with the same procedure, which is given here directly as

$$\tilde{\mathbf{M}}\ddot{\tilde{\mathbf{x}}} + \tilde{\mathbf{C}}\dot{\tilde{\mathbf{x}}} + \tilde{\mathbf{K}}\tilde{\mathbf{x}} = \tilde{\mathbf{f}} \tag{40}$$

where $\tilde{\mathbf{M}}$ is the equivalent mass matrix of the reduced system; $\tilde{\mathbf{C}}$ and $\tilde{\mathbf{K}}$ are the equivalent time-variant damping and stiffness matrices of the reduced system, respectively; $\tilde{\mathbf{f}}$ is the equivalent force vector of the reduced system; and $\ddot{\tilde{\mathbf{x}}}$, $\dot{\tilde{\mathbf{x}}}$ and $\tilde{\mathbf{x}}$ are respectively the equivalent acceleration, velocity and displacement vectors of the reduced system. These variables are expressed as

$$\tilde{\mathbf{M}} = \begin{bmatrix} \mathbf{I}_m^L + \left[\mathbf{T}^L\right]^T \mathbf{M}^L\mathbf{T}^L & \left[\mathbf{T}^L\right]^T \mathbf{M}^L\mathbf{T}^N \\ \left[\mathbf{T}^N\right]^T \mathbf{M}^L\mathbf{T}^L & \mathbf{M}^N + \left[\mathbf{T}^N\right]^T \mathbf{M}^L\mathbf{T}^N \end{bmatrix} \tag{41}$$

$$\tilde{\mathbf{K}} = \begin{bmatrix} \mathbf{\Lambda}_m^L + \left[\mathbf{T}^L\right]^T \mathbf{K}^L \mathbf{T}^L & \left[\mathbf{T}^L\right]^T \mathbf{K}^L \mathbf{T}^N \\ \left[\mathbf{T}^N\right]^T \mathbf{K}^L \mathbf{T}^L & \mathbf{K}^N + \left[\mathbf{T}^N\right]^T \mathbf{K}^L \mathbf{T}^N \end{bmatrix} \tag{42}$$

$$\tilde{\mathbf{C}} = a_1 \tilde{\mathbf{M}} + a_2 \tilde{\mathbf{K}} \tag{43}$$

$$\tilde{\mathbf{f}} = \begin{Bmatrix} \left(\mathbf{\Phi}_m^L - \mathbf{T}^L\right)^T \mathbf{f}^L + \left[\mathbf{T}^L\right]^T \mathbf{M}^L \mathbf{S}\left(a_1 \dot{\mathbf{f}}^L + \ddot{\mathbf{f}}^L\right) \\ \mathbf{f}^N - \left[\mathbf{T}^N\right]^T \mathbf{f}^L + \left[\mathbf{T}^N\right]^T \mathbf{M}^L \mathbf{S}\left(a_1 \dot{\mathbf{f}}^L + \ddot{\mathbf{f}}^L\right) \end{Bmatrix} \tag{44}$$

$$\tilde{\mathbf{x}} = \begin{Bmatrix} \mathbf{z}_m^L \\ \mathbf{x}^N \end{Bmatrix}, \quad \dot{\tilde{\mathbf{x}}} = \begin{Bmatrix} \dot{\mathbf{z}}_m^L \\ \dot{\mathbf{x}}^N \end{Bmatrix}, \quad \ddot{\tilde{\mathbf{x}}} = \begin{Bmatrix} \ddot{\mathbf{z}}_m^L \\ \ddot{\mathbf{x}}^N \end{Bmatrix} \tag{45}$$

where $\dot{\mathbf{f}}^L$ is the first-order derivative of $\mathbf{f}^L$ with respect to time *t*. It can be calculated with the finite difference method or derived directly.

The reduced vibration equation (Eq. (40)) can be solved using classical numerical integration methods like Newmark-β method or Wilson-θ method with an iterative scheme. In each time step, an iterative process is performed to determine the time-variant matrices $\tilde{\mathbf{K}}$ and $\tilde{\mathbf{C}}$. Eq. (40) is composed of the linear and nonlinear parts. The size of the linear parts is reduced to the total number of the master modes of linear substructures, which is subsequently combined with the small-size local nonlinear parts. In consequence, the system matrices in Eq. (40) have the order of $\left(\sum_{j=1}^{NL} m^{(j)} + \sum_{k=NL+1}^{NS} n^{(k)}\right)$, which is much smaller than that of the global system of *n*. The calculation of structural responses from the reduced vibration equation can save plenty of time. The structural responses of the nonlinear substructures $\mathbf{x}^N$, $\dot{\mathbf{x}}^N$ and $\ddot{\mathbf{x}}^N$ can be extracted directly from Eq. (45). According to Eqs. (15) and (37), the structural responses of the linear substructures $\mathbf{x}^L$, $\dot{\mathbf{x}}^L$ and $\ddot{\mathbf{x}}^L$ are calculated by

$$\mathbf{x}^L = \mathbf{\Phi}^L \mathbf{z}^L = \mathbf{\Phi}_m^L \mathbf{z}_m^L + \mathbf{\Phi}_s^L \mathbf{z}_s^L = \left(\mathbf{\Phi}_m^L - \mathbf{T}^L\right)\mathbf{z}_m^L - \mathbf{T}^N \mathbf{x}^N + \mathbf{S}\mathbf{f}^L \tag{46}$$

$$\dot{\mathbf{x}}^L = \mathbf{\Phi}_m^L \dot{\mathbf{z}}_m^L + \mathbf{\Phi}_s^L \dot{\mathbf{z}}_s^L = \left(\mathbf{\Phi}_m^L - \mathbf{T}^L\right)\dot{\mathbf{z}}_m^L - \mathbf{T}^N \dot{\mathbf{x}}^N + \mathbf{S}\dot{\mathbf{f}}^L \tag{47}$$

$$\ddot{\mathbf{x}}^L = \mathbf{\Phi}_m^L \ddot{\mathbf{z}}_m^L + \mathbf{\Phi}_s^L \ddot{\mathbf{z}}_s^L = \left(\mathbf{\Phi}_m^L - \mathbf{T}^L\right)\ddot{\mathbf{z}}_m^L - \mathbf{T}^N \ddot{\mathbf{x}}^N + \mathbf{S}\ddot{\mathbf{f}}^L \tag{48}$$

Finally, the responses of the global structure are obtained directly by merging the identical values at the interface DOFs.

3. Substructuring method for response sensitivities of nonlinear systems

The response sensitivities are the derivatives of the structural responses with respect to the design parameters. The design parameters can be either the linear or nonlinear parameters. Based on the reduced vibration equation (Eq. (40)), the response sensitivities can be calculated by various methods including the finite difference method, perturbation method, adjoint method and direct differentiation method. Compared to the former three methods with different limitations, the direct differentiation ~~latter~~ method derives the response sensitivity from the vibration equation directly, which is efficient, accurate and general for various nonlinear problems [35]. So, in this section, the direct differentiation method is employed to derive the first-order derivative of the structural responses with respect to a design parameter *r* from the reduced system vibration equation Eq. (40).

Differentiating Eq. (40) with respect to *r* leads to

$$\tilde{\mathbf{M}}\frac{\partial \ddot{\tilde{\mathbf{x}}}}{\partial r} + \tilde{\mathbf{C}}\frac{\partial \dot{\tilde{\mathbf{x}}}}{\partial r} + \tilde{\mathbf{K}}\frac{\partial \tilde{\mathbf{x}}}{\partial r} = \frac{\partial \tilde{\mathbf{f}}}{\partial r} - \frac{\partial \tilde{\mathbf{M}}}{\partial r}\ddot{\tilde{\mathbf{x}}} - \frac{\partial \tilde{\mathbf{C}}}{\partial r}\dot{\tilde{\mathbf{x}}} - \frac{\partial \tilde{\mathbf{K}}}{\partial r}\tilde{\mathbf{x}} \tag{49}$$

where $\frac{\partial \tilde{\mathbf{x}}}{\partial r}$, $\frac{\partial \dot{\tilde{\mathbf{x}}}}{\partial r}$ and $\frac{\partial \ddot{\tilde{\mathbf{x}}}}{\partial r}$ have the form of

$$\frac{\partial \tilde{\mathbf{x}}}{\partial r} = \begin{Bmatrix} \frac{\partial \mathbf{z}_m^L}{\partial r} \\ \frac{\partial \mathbf{x}^N}{r} \end{Bmatrix}, \quad \frac{\partial \dot{\tilde{\mathbf{x}}}}{\partial r} = \begin{Bmatrix} \frac{\partial \dot{\mathbf{z}}_m^L}{\partial r} \\ \frac{\partial \dot{\mathbf{x}}^N}{\partial r} \end{Bmatrix}, \quad \frac{\partial \ddot{\tilde{\mathbf{x}}}}{\partial r} = \begin{Bmatrix} \frac{\partial \ddot{\mathbf{z}}_m^L}{\partial r} \\ \frac{\partial \ddot{\mathbf{x}}^N}{\partial r} \end{Bmatrix} \tag{50}$$

Since the response sensitivities are usually calculated together with the structural responses, the variables obtained in the previous section, such as $\tilde{\mathbf{M}}$, $\tilde{\mathbf{C}}$, $\tilde{\mathbf{K}}$, $\ddot{\tilde{\mathbf{x}}}$, $\dot{\tilde{\mathbf{x}}}$ and $\tilde{\mathbf{x}}$, can be reused here directly. Once $\frac{\partial \tilde{\mathbf{M}}}{\partial r}$, $\frac{\partial \tilde{\mathbf{K}}}{\partial r}$, $\frac{\partial \tilde{\mathbf{C}}}{\partial r}$ and $\frac{\partial \tilde{\mathbf{f}}}{\partial r}$ are available, Eq. (49) can be calculated with numerical integration methods like Newmark-β method or Wilson-θ method.

$\frac{\partial \tilde{\mathbf{M}}}{\partial r}$, $\frac{\partial \tilde{\mathbf{K}}}{\partial r}$, $\frac{\partial \tilde{\mathbf{C}}}{\partial r}$ and $\frac{\partial \tilde{\mathbf{f}}}{\partial r}$ are calculated by differentiating Eqs. (41)-(44) with respect to r,

$$\frac{\partial \tilde{\mathbf{M}}}{\partial r} = \begin{bmatrix} \left[\frac{\partial \mathbf{T}^L}{\partial r}\right]^T \mathbf{M}^L \mathbf{T}^L + \left[\mathbf{T}^L\right]^T \frac{\partial \mathbf{M}^L}{\partial r} \mathbf{T}^L + \left[\mathbf{T}^L\right]^T \mathbf{M}^L \frac{\partial \mathbf{T}^L}{\partial r} & \left[\frac{\partial \mathbf{T}^L}{\partial r}\right]^T \mathbf{M}^L \mathbf{T}^N + \left[\mathbf{T}^L\right]^T \frac{\partial \mathbf{M}^L}{\partial r} \mathbf{T}^N + \left[\mathbf{T}^L\right]^T \mathbf{M}^L \frac{\partial \mathbf{T}^N}{\partial r} \\ \left[\frac{\partial \mathbf{T}^N}{\partial r}\right]^T \mathbf{M}^L \mathbf{T}^L + \left[\mathbf{T}^N\right]^T \frac{\partial \mathbf{M}^L}{\partial r} \mathbf{T}^L + \left[\mathbf{T}^N\right]^T \mathbf{M}^L \frac{\partial \mathbf{T}^L}{\partial r} & \frac{\partial \mathbf{M}^N}{\partial r} + \left[\frac{\partial \mathbf{T}^N}{\partial r}\right]^T \mathbf{M}^L \mathbf{T}^N + \left[\mathbf{T}^N\right]^T \frac{\partial \mathbf{M}^L}{\partial r} \mathbf{T}^N + \left[\mathbf{T}^N\right]^T \mathbf{M}^L \frac{\partial \mathbf{T}^N}{\partial r} \end{bmatrix} \tag{51}$$

$$\frac{\partial \tilde{\mathbf{K}}}{\partial r} = \begin{bmatrix} \frac{\partial \boldsymbol{\Lambda}_m^L}{\partial r} + \left[\frac{\partial \mathbf{T}^L}{\partial r}\right]^T \mathbf{K}^L \mathbf{T}^L + \left[\mathbf{T}^L\right]^T \frac{\partial \mathbf{K}^L}{\partial r} \mathbf{T}^L + \left[\mathbf{T}^L\right]^T \mathbf{K}^L \frac{\partial \mathbf{T}^L}{\partial r} & \left[\frac{\partial \mathbf{T}^L}{\partial r}\right]^T \mathbf{K}^L \mathbf{T}^N + \left[\mathbf{T}^L\right]^T \frac{\partial \mathbf{K}^L}{\partial r} \mathbf{T}^N + \left[\mathbf{T}^L\right]^T \mathbf{K}^L \frac{\partial \mathbf{T}^N}{\partial r} \\ \left[\frac{\partial \mathbf{T}^N}{\partial r}\right]^T \mathbf{K}^L \mathbf{T}^L + \left[\mathbf{T}^N\right]^T \frac{\partial \mathbf{K}^L}{\partial r} \mathbf{T}^L + \left[\mathbf{T}^N\right]^T \mathbf{K}^L \frac{\partial \mathbf{T}^L}{\partial r} & \frac{\partial \mathbf{K}^N}{\partial r} + \left[\frac{\partial \mathbf{T}^N}{\partial r}\right]^T \mathbf{K}^L \mathbf{T}^N + \left[\mathbf{T}^N\right]^T \frac{\partial \mathbf{K}^L}{\partial r} \mathbf{T}^N + \left[\mathbf{T}^N\right]^T \mathbf{K}^L \frac{\partial \mathbf{T}^N}{\partial r} \end{bmatrix} \tag{52}$$

$$\frac{\partial \tilde{\mathbf{C}}}{\partial r} = a_1 \frac{\partial \tilde{\mathbf{M}}}{\partial r} + a_2 \frac{\partial \tilde{\mathbf{K}}}{\partial r} \tag{53}$$

$$\frac{\partial \tilde{\mathbf{f}}}{\partial r}=\left\{\begin{array}{l}\left(\frac{\partial \mathbf{\Phi}_m^L}{\partial r}-\frac{\partial \mathbf{T}^L}{\partial r}\right)^T\mathbf{f}^L+\left(\left[\frac{\partial \mathbf{T}^L}{\partial r}\right]^T\mathbf{M}^L\mathbf{S}+\left[\mathbf{T}^L\right]^T\frac{\partial \mathbf{M}^L}{\partial r}\mathbf{S}+\left[\mathbf{T}^L\right]^T\mathbf{M}^L\frac{\partial \mathbf{S}}{\partial r}\right)\left(a_1\dot{\mathbf{f}}^L+\ddot{\mathbf{f}}^L\right)\\ -\left[\frac{\partial \mathbf{T}^N}{\partial r}\right]^T\mathbf{f}^L+\left(\left[\frac{\partial \mathbf{T}^N}{\partial r}\right]^T\mathbf{M}^L\mathbf{S}+\left[\mathbf{T}^N\right]^T\frac{\partial \mathbf{M}^L}{\partial r}\mathbf{S}+\left[\mathbf{T}^N\right]^T\mathbf{M}^L\frac{\partial \mathbf{S}}{\partial r}\right)\left(a_1\dot{\mathbf{f}}^L+\ddot{\mathbf{f}}^L\right)\end{array}\right\} \tag{54}$$

In Eqs. (51)-(54), $\frac{\partial \mathbf{T}^L}{\partial r}$, $\frac{\partial \mathbf{T}^N}{\partial r}$ and $\frac{\partial \mathbf{S}}{\partial r}$ are calculated by differentiating Eqs. (34)-(36) with respect to r as

$$\begin{aligned}\frac{\partial \mathbf{T}^L}{\partial r}=&\frac{\partial \mathbf{F}^L}{\partial r}\left[\mathbf{D}^L\right]^T\left(\mathbf{D}^L\mathbf{F}^L\left[\mathbf{D}^L\right]^T\right)^{-1}\mathbf{D}^L\mathbf{\Phi}_m^L-\mathbf{F}^L\left[\mathbf{D}^L\right]^T\left(\mathbf{D}^L\mathbf{F}^L\left[\mathbf{D}^L\right]^T\right)^{-1}\mathbf{D}^L\frac{\partial \mathbf{F}^L}{\partial r}\left[\mathbf{D}^L\right]^T\left(\mathbf{D}^L\mathbf{F}^L\left[\mathbf{D}^L\right]^T\right)^{-1}\mathbf{D}^L\mathbf{\Phi}_m^L\\&+\mathbf{F}^L\left[\mathbf{D}^L\right]^T\left(\mathbf{D}^L\mathbf{F}^L\left[\mathbf{D}^L\right]^T\right)^{-1}\mathbf{D}^L\frac{\partial \mathbf{\Phi}_m^L}{\partial r}\end{aligned} \tag{55}$$

$$\frac{\partial \mathbf{T}^N}{\partial r}=\frac{\partial \mathbf{F}^L}{\partial r}\left[\mathbf{D}^L\right]^T\left(\mathbf{D}^L\mathbf{F}^L\left[\mathbf{D}^L\right]^T\right)^{-1}\mathbf{D}^N-\mathbf{F}^L\left[\mathbf{D}^L\right]^T\left(\mathbf{D}^L\mathbf{F}^L\left[\mathbf{D}^L\right]^T\right)^{-1}\left(\mathbf{D}^L\frac{\partial \mathbf{F}^L}{\partial r}\left[\mathbf{D}^L\right]^T\right)\left(\mathbf{D}^L\mathbf{F}^L\left[\mathbf{D}^L\right]^T\right)^{-1}\mathbf{D}^N \tag{56}$$

$$\begin{aligned}\frac{\partial \mathbf{S}}{\partial r}=&\frac{\partial \mathbf{F}^L}{\partial r}-\frac{\partial \mathbf{F}^L}{\partial r}\left[\mathbf{D}^L\right]^T\left(\mathbf{D}^L\mathbf{F}^L\left[\mathbf{D}^L\right]^T\right)^{-1}\mathbf{D}^L\mathbf{F}^L+\mathbf{F}^L\left[\mathbf{D}^L\right]^T\left(\mathbf{D}^L\mathbf{F}^L\left[\mathbf{D}^L\right]^T\right)^{-1}\mathbf{D}^L\frac{\partial \mathbf{F}^L}{\partial r}\left[\mathbf{D}^L\right]^T\left(\mathbf{D}^L\mathbf{F}^L\left[\mathbf{D}^L\right]^T\right)^{-1}\mathbf{D}^L\mathbf{F}^L\\&-\mathbf{F}^L\left[\mathbf{D}^L\right]^T\left(\mathbf{D}^L\mathbf{F}^L\left[\mathbf{D}^L\right]^T\right)^{-1}\mathbf{D}^L\frac{\partial \mathbf{F}^L}{\partial r}\end{aligned} \tag{57}$$

Each substructure is treated as an independent structure, the time-invariant derivative matrices $\frac{\partial \mathbf{M}^N}{\partial r}$, $\frac{\partial \mathbf{K}^L}{\partial r}$, $\frac{\partial \mathbf{M}^L}{\partial r}$, $\frac{\partial \mathbf{F}^L}{\partial r}$, $\frac{\partial \mathbf{\Lambda}_m^L}{\partial r}$ and $\frac{\partial \mathbf{\Phi}_m^L}{\partial r}$ are therefore zeros except for the specific substructure containing r. If r is located in a linear substructure (for example, the A^{th} substructure), $\frac{\partial \mathbf{M}^N}{\partial r}=\mathbf{0}$. $\frac{\partial \mathbf{K}^L}{\partial r}$, $\frac{\partial \mathbf{M}^L}{\partial r}$, $\frac{\partial \mathbf{F}^L}{\partial r}$, $\frac{\partial \mathbf{\Lambda}_m^L}{\partial r}$ and $\frac{\partial \mathbf{\Phi}_m^L}{\partial r}$

are related to the derivative matrices of the A^{th} substructure solely, and expressed in the form of

$$\frac{\partial \mathbf{K}^{L}}{\partial r}=diag\left(\mathbf{0}\ \cdots\ \frac{\partial \mathbf{K}^{(A)}}{\partial r}\ \cdots\ \mathbf{0}\right),\ \frac{\partial \mathbf{M}^{L}}{\partial r}=diag\left(\mathbf{0}\ \cdots\ \frac{\partial \mathbf{M}^{(A)}}{\partial r}\ \cdots\ \mathbf{0}\right),$$
$$\frac{\partial \mathbf{F}^{L}}{\partial r}=diag\left(\mathbf{0}\ \cdots\ \frac{\partial \mathbf{F}^{(A)}}{\partial r}\ \cdots\ \mathbf{0}\right),\ \frac{\partial \mathbf{\Lambda}_{m}^{L}}{\partial r}=diag\left(\mathbf{0}\ \cdots\ \frac{\partial \mathbf{\Lambda}_{m}^{(A)}}{\partial r}\ \cdots\ \mathbf{0}\right),$$
$$\frac{\partial \mathbf{\Phi}_{m}^{L}}{\partial r}=diag\left(\mathbf{0}\ \cdots\ \frac{\partial \mathbf{\Phi}_{m}^{(A)}}{\partial r}\ \cdots\ \mathbf{0}\right) \tag{58}$$

where the derivative of the residual flexibility matrix of the A^{th} substructure $\frac{\partial \mathbf{F}^{(A)}}{\partial r}$ is calculated by [31]

$$\begin{aligned}\frac{\partial \mathbf{F}^{(A)}}{\partial r}=&-\left[\mathbf{K}^{(A)}\right]^{-1}\frac{\partial \mathbf{K}^{(A)}}{\partial r}\left[\mathbf{K}^{(A)}\right]^{-1}-\frac{\partial \mathbf{\Phi}_{m}^{(A)}}{\partial r}\left[\mathbf{\Lambda}_{m}^{(A)}\right]^{-1}\left[\mathbf{\Phi}_{m}^{(A)}\right]^{T}+\mathbf{\Phi}_{m}^{(A)}\left[\mathbf{\Lambda}_{m}^{(A)}\right]^{-1}\frac{\partial \mathbf{\Lambda}_{m}^{(A)}}{\partial r}\left[\mathbf{\Lambda}_{m}^{(A)}\right]^{-1}\left[\mathbf{\Phi}_{m}^{(A)}\right]^{T}\\&-\mathbf{\Phi}_{m}^{(A)}\left[\mathbf{\Lambda}_{m}^{(A)}\right]^{-1}\left[\frac{\partial \mathbf{\Phi}_{m}^{(A)}}{\partial r}\right]^{T}\end{aligned} \tag{59}$$

$\frac{\partial \mathbf{K}^{(A)}}{\partial r}$ and $\frac{\partial \mathbf{M}^{(A)}}{\partial r}$ can be calculated directly from the elemental stiffness and mass matrices associated with *r*. $\frac{\partial \mathbf{\Lambda}_{m}^{(A)}}{\partial r}$ and $\frac{\partial \mathbf{\Phi}_{m}^{(A)}}{\partial r}$ can be calculated within the A^{th} substructure by employing the traditional methods like Rogers' method [36] or Nelson's method [37].

On the other hand, if *r* is located in a nonlinear substructure (for example the B^{th} substructure), the time-invariant derivative matrices associated with the linear substructures are zeros, that is $\frac{\partial \mathbf{K}^L}{\partial r}$, $\frac{\partial \mathbf{M}^L}{\partial r}$, $\frac{\partial \mathbf{F}^L}{\partial r}$, $\frac{\partial \mathbf{\Lambda}_m^L}{\partial r}$ and $\frac{\partial \mathbf{\Phi}_m^L}{\partial r}$ are zeros. The derivative matrices $\frac{\partial \mathbf{T}^L}{\partial r}$, $\frac{\partial \mathbf{T}^N}{\partial r}$ and $\frac{\partial \mathbf{S}}{\partial r}$ are zeros as a consequence. $\frac{\partial \mathbf{M}^N}{\partial r}$ are zeros except for the B^{th} substructure, that is

$$\frac{\partial \mathbf{M}^N}{\partial r} = diag\begin{pmatrix} \mathbf{0} & \cdots & \frac{\partial \mathbf{M}^{(B)}}{\partial r} & \cdots & \mathbf{0} \end{pmatrix} \tag{60}$$

The derivative matrix $\frac{\partial \mathbf{M}^{(B)}}{\partial r}$ can be derived directly from the specific elemental matrix containing r. $\frac{\partial \tilde{\mathbf{M}}}{\partial r}$, $\frac{\partial \tilde{\mathbf{K}}}{\partial r}$ and $\frac{\partial \tilde{\mathbf{f}}}{\partial r}$ are then simplified into

$$\frac{\partial \tilde{\mathbf{M}}}{\partial r} = \begin{bmatrix} \mathbf{0} & \mathbf{0} \\ \mathbf{0} & \frac{\partial \mathbf{M}^N}{\partial r} \end{bmatrix},\ \frac{\partial \tilde{\mathbf{K}}}{\partial r} = \begin{bmatrix} \mathbf{0} & \mathbf{0} \\ \mathbf{0} & \frac{\partial \mathbf{K}^N}{\partial r} \end{bmatrix},\ \frac{\partial \tilde{\mathbf{f}}}{\partial r} = \{\mathbf{0}\} \tag{61}$$

When the design parameter is located in the nonlinear substructure, calculation of the derivative matrices is directly performed on one specific nonlinear substructure, and simpler than when the parameter is in the linear substructure.

The final unknown variable in Eqs. (49)-(54) is $\frac{\partial \mathbf{K}^N}{\partial r}$. As $\mathbf{K}^N$ is the function of $\mathbf{x}^N$ (see Eq. (6)), $\frac{\partial \mathbf{K}^N}{\partial r}$ is the function of $\mathbf{x}^N$ and $\frac{\partial \mathbf{x}^N}{\partial r}$. $\mathbf{x}^N$ is available in the calculation of structural responses. $\frac{\partial \mathbf{x}^N}{\partial r}$ can be extracted directly from $\frac{\partial \tilde{\mathbf{x}}}{\partial r}$ in Eq. (50). Eq. (49) can thus be calculated with numerical integration methods with an iterative scheme. In each time step, an iterative process is performed to search for the accurate time-variant matrix $\frac{\partial \mathbf{K}^N}{\partial r}$.

After $\frac{\partial \ddot{\tilde{\mathbf{x}}}}{\partial r}$, $\frac{\partial \dot{\tilde{\mathbf{x}}}}{\partial r}$ and $\frac{\partial \tilde{\mathbf{x}}}{\partial r}$ are solved from Eq. (49), the response sensitivities at the nonlinear substructures can be extracted directly from Eq. (50). The response sensitivities at the linear substructures are computed by differentiating Eqs. (46)-(48) with respect to *r*

$$\frac{\partial \mathbf{x}^L}{\partial r} = \left(\frac{\partial \mathbf{\Phi}_m^L}{\partial r} - \frac{\partial \mathbf{T}^L}{\partial r} \right) \mathbf{z}_m^L + \left(\mathbf{\Phi}_m^L - \mathbf{T}^L \right) \frac{\partial \mathbf{z}_m^L}{\partial r} - \frac{\partial \mathbf{T}^N}{\partial r} \mathbf{x}^N - \mathbf{T}^N \frac{\partial \mathbf{x}^N}{\partial r} + \frac{\partial \mathbf{S}}{\partial r} \mathbf{f}^L \tag{62}$$

$$\frac{\partial \dot{\mathbf{x}}^L}{\partial r} = \left(\frac{\partial \mathbf{\Phi}_m^L}{\partial r} - \frac{\partial \mathbf{T}^L}{\partial r} \right) \dot{\mathbf{z}}_m^L + \left(\mathbf{\Phi}_m^L - \mathbf{T}^L \right) \frac{\partial \dot{\mathbf{z}}_m^L}{\partial r} - \frac{\partial \mathbf{T}^N}{\partial r} \dot{\mathbf{x}}^N - \mathbf{T}^N \frac{\partial \dot{\mathbf{x}}^N}{\partial r} + \frac{\partial \mathbf{S}}{\partial r} \dot{\mathbf{f}}^L \tag{63}$$

$$\frac{\partial \ddot{\mathbf{x}}^L}{\partial r} = \left(\frac{\partial \mathbf{\Phi}_m^L}{\partial r} - \frac{\partial \mathbf{T}^L}{\partial r} \right) \ddot{\mathbf{z}}_m^L + \left(\mathbf{\Phi}_m^L - \mathbf{T}^L \right) \frac{\partial \ddot{\mathbf{z}}_m^L}{\partial r} - \frac{\partial \mathbf{T}^N}{\partial r} \ddot{\mathbf{x}}^N - \mathbf{T}^N \frac{\partial \ddot{\mathbf{x}}^N}{\partial r} + \frac{\partial \mathbf{S}}{\partial r} \ddot{\mathbf{f}}^L \tag{64}$$

Finally, the response sensitivities of the global structure are obtained directly by merging the identical values at the interface DOFs.

Different from the traditional method that computes the response sensitivities from the global vibration equation, the proposed method derives the response sensitivities from the reduced vibration equation Eq. (40) of a much smaller size. It is expected that the proposed method is more efficient than the global method especially for large-scale structures.

4. Case study 1: a nonlinear spring-mass system

A simple nonlinear spring-mass system (as shown in Figure 1) with 5 DOFs is first employed to demonstrate the proposed substructuring method in detail. The five masses are m_1=100 kg, m_2=200 kg, m_3=150 kg, m_4=200 kg, and m_5=200 kg. The masses are connected by five linear springs and a nonlinear spring. The stiffness parameters of the five linear springs are k_1=k_2=1000 N/m, k_3=k_4=2000 N/m, k_5=500 N/m. m_4 and m_5 are also connected with a nonlinear spring, which has a k_s=2×10^5 N/m^3 and a cubic restoring force $F_s=-k_s(\Delta x)^3=-k_{\text{non}}(x)\Delta x$, where Δx is the relative displacements of m_5 and m_4 ($\Delta x=x_5-x_4$). $k_{\text{non}}(x)= k_s(\Delta x)^2$ is the time-variant equivalent stiffness of the nonlinear spring. The Rayleigh damping is assumed for the system with the damping coefficients of a_1=0.0508 s^{-1} and a_2=0.0396 s. The system is subject to a harmonic acceleration excitation $\ddot{x}_g = 0.5\sin\left(2\pi t\right)\text{m}/\text{s}^2 \left(0 \le t \le 20\text{s}\right)$. The excitation is discretized into 10,000 time steps of 0.002 s to compute the structural responses and response sensitivities. The change ratio of k_2 is selected as the design parameter, which is denoted as r_1.

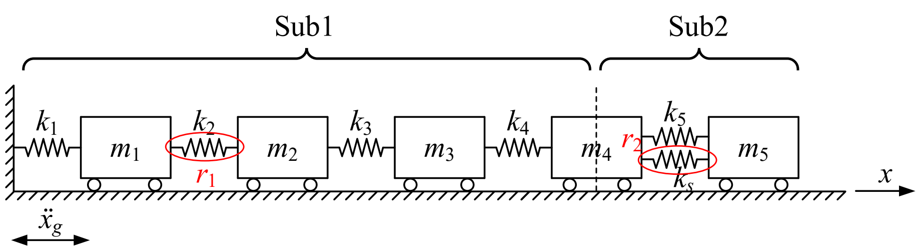

Figure 1. A nonlinear spring-mass system.

The nonlinearity may be unknown in advance for a practical structure. The presence and location of the nonlinearity are thus required to be identified. Many methods have been developed for the localization of the nonlinearities [1, 2, 38]. Here the ordinary coherence function is used to detect the presence and location of nonlinearity by assessing the quality of data measured under the external excitation as [2, 39]

$$\gamma^2(\omega) = \frac{\left|S_{yx}(\omega)\right|^2}{S_{xx}(\omega) S_{yy}(\omega)} = \frac{H_1(\omega)}{H_2(\omega)} \tag{65}$$

where $H_1(\omega) = \frac{S_{yx}(\omega)}{S_{xx}(\omega)}$ and $H_2(\omega) = \frac{S_{yy}(\omega)}{S_{yx}(\omega)}$ are respectively the so-called H_1 and H_2 frequency response function estimator. $S_{yy}(\omega)$, $S_{xx}(\omega)$, $S_{yx}(\omega)$ denote the power spectral density (PSD) of the response, the PSD of the imposed force and the cross PSD between the response and the imposed force. The ordinary coherence function is expected to be unity for all accessible frequencies if and only if the system is linear and noise-free. It is a fast and effective detection tool for nonlinear behavior in a specific frequency bands [40].

The structural responses are first calculated directly from the global structure using the Newmark method and Newton-Raphson iteration method [39]. The calculated responses serve as the measured data to detect the presence and location of nonlinearity. The ordinary coherence functions of the imposed force with respect to the measured acceleration of m_1~m_5 are displayed in Figure 2. The corresponding ordinary coherence functions for m_4 and m_5 are quite discrepant from 1 while those of m_1~m_3 are close to 1, which indicates strong nonlinearities at m_4 and m_5.

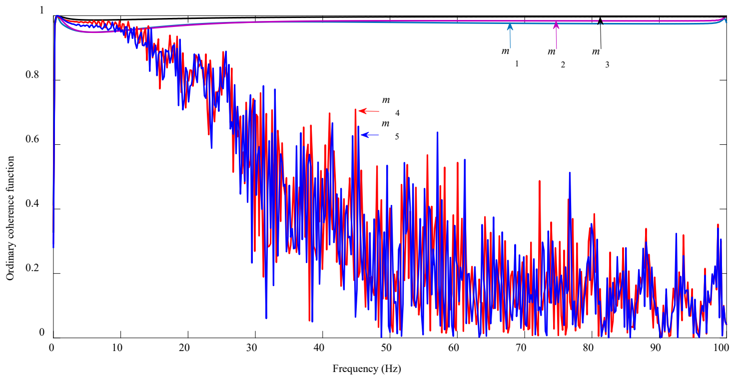

Figure 2. Ordinary coherence functions of m_1~m_5.

The proposed substructuring method is then employed to calculate the structural responses and response sensitivities of this nonlinear system as follows:

1) The system is divided into two substructures based on the nonlinearity identification results, as shown in Figure 1. The first substructure is a linear substructure consisting of four DOFs and the second is a nonlinear substructure with two DOFs. After division, the assembled mass and stiffness matrices of the linear substructure are

$$\mathbf{M}^L = \begin{bmatrix} 100 & 0 & 0 & 0 \\ 0 & 200 & 0 & 0 \\ 0 & 0 & 150 & 0 \\ 0 & 0 & 0 & 100 \end{bmatrix}, \quad \mathbf{K}^L = \begin{bmatrix} 2000 & -1000 & 0 & 0 \\ -1000 & 3000 & -2000 & 0 \\ 0 & -2000 & 4000 & -2000 \\ 0 & 0 & -2000 & 2000 \end{bmatrix}$$

The assembled mass and stiffness matrices of the nonlinear substructure are

$$\mathbf{M}^N = \begin{bmatrix} 100 & 0 \\ 0 & 200 \end{bmatrix}, \quad \mathbf{K}^N = \begin{bmatrix} 500 + k_{\text{non}}(x) & -500 - k_{\text{non}}(x) \\ -500 - k_{\text{non}}(x) & 500 + k_{\text{non}}(x) \end{bmatrix}$$

The derivative matrices associated with the linear substructure are

$$\frac{\partial \mathbf{M}^L}{\partial r_1} = \mathbf{0}, \quad \frac{\partial \mathbf{K}^L}{\partial r_1} = \begin{bmatrix} 1000 & -1000 & 0 & 0 \\ -1000 & 1000 & 0 & 0 \\ 0 & 0 & 0 & 0 \\ 0 & 0 & 0 & 0 \end{bmatrix}$$

The derivative matrices associated with the nonlinear substructure are

$$\frac{\partial \mathbf{M}^N}{\partial r_1} = \mathbf{0}, \quad \frac{\partial \mathbf{K}^N}{\partial r_1} = \begin{bmatrix} \frac{\partial k_{\text{non}}(x)}{\partial r_1} & -\frac{\partial k_{\text{non}}(x)}{\partial r_1} \\ -\frac{\partial k_{\text{non}}(x)}{\partial r_1} & \frac{\partial k_{\text{non}}(x)}{\partial r_1} \end{bmatrix}$$

where $\frac{\partial k_{\text{non}}(x)}{\partial r_1} = 2k_s(x_5 - x_4)\left(\frac{\partial x_5}{\partial r_1} - \frac{\partial x_4}{\partial r_1}\right)$ is a time-variant variable. The connection matrix **D** is constructed as

$$\mathbf{D} = \begin{bmatrix} 0 & 0 & 0 & 1 & -1 & 0 \end{bmatrix}$$

The component matrices of $\mathbf{D}$ associated with the linear and nonlinear substructures are

$$\mathbf{D}^L = \begin{bmatrix} 0 & 0 & 0 & 1 \end{bmatrix}, \quad \mathbf{D}^N = \begin{bmatrix} -1 & 0 \end{bmatrix}$$

The external excitation of the linear substructure and nonlinear substructure are

$$\mathbf{f}^L = -\mathbf{M}^L \mathbf{I}_{4\times 4} \ddot{x}_g, \quad \mathbf{f}^N = -\mathbf{M}^N \mathbf{I}_{2\times 2} \ddot{x}_g$$

2) The first three modes are selected as the master modes for the linear substructure, the master eigenvalues $\mathbf{\Lambda}_m^{(1)}$ and eigenvectors $\mathbf{\Phi}_m^{(1)}$ of the linear substructure are solved from the eigen-equation $\mathbf{K}^{(1)}\mathbf{\Phi}_m^{(1)} = \mathbf{\Lambda}_m^{(1)}\mathbf{M}^{(1)}\mathbf{\Phi}_m^{(1)}$. r_1 is located in the first substructure. The derivatives of the master eigenvalues $\frac{\partial \mathbf{\Lambda}_m^{(1)}}{\partial r_1}$ and eigenvectors $\frac{\partial \mathbf{\Phi}_m^{(1)}}{\partial r_1}$ are calculated by employing Nelson's method [37]. $\mathbf{\Lambda}_m^L$, $\mathbf{\Phi}_m^L$, $\frac{\partial \mathbf{\Lambda}_m^L}{\partial r_1}$ and $\frac{\partial \mathbf{\Phi}_m^L}{\partial r_1}$ are diagonally assembled from the corresponding matrices of all linear substructures. This example has only one linear substructure, accordingly $\mathbf{\Lambda}_m^L = \mathbf{\Lambda}_m^{(1)}$, $\mathbf{\Phi}_m^L = \mathbf{\Phi}_m^{(1)}$, $\frac{\partial \mathbf{\Lambda}_m^L}{\partial r_1} = \frac{\partial \mathbf{\Lambda}_m^{(1)}}{\partial r_1}$ and $\frac{\partial \mathbf{\Phi}_m^L}{\partial r_1} = \frac{\partial \mathbf{\Phi}_m^{(1)}}{\partial r_1}$.

$$\mathbf{\Lambda}_m^L = \begin{bmatrix} 0.9667 & 0 & 0 \\ 0 & 13.0912 & 0 \\ 0 & 0 & 24.3617 \end{bmatrix}, \quad \mathbf{\Phi}_m^L = \begin{bmatrix} -0.02208 & 0.05510 & 0.07981 \\ -0.04202 & 0.03807 & -0.03481 \\ -0.04793 & -0.02028 & -0.007316 \\ -0.05036 & -0.05872 & 0.03355 \end{bmatrix}$$

$$\frac{\partial \mathbf{\Lambda}_m^L}{\partial r_1} = \begin{bmatrix} 0.3977 & 0 & 0 \\ 0 & 0.2901 & 0 \\ 0 & 0 & 13.1394 \end{bmatrix}, \quad \frac{\partial \mathbf{\Phi}_m^L}{\partial r_1} = \begin{bmatrix} -0.009509 & -0.014645 & 0.005248 \\ 0.002722 & 0.005317 & 0.007467 \\ 0.0002738 & -0.001284 & -0.021185 \\ -0.0007645 & -0.006183 & -0.003919 \end{bmatrix}$$

3) The residual flexibility of the linear substructure $\mathbf{F}^L$ is calculated from Eq. (32).

The intermediate variables $\mathbf{T}^L$, $\mathbf{T}^N$ and $\mathbf{S}$ are calculated by Eqs. (34)-(36). The derivative matrices $\frac{\partial \mathbf{F}^L}{\partial r_1}$, $\frac{\partial \mathbf{T}^L}{\partial r_1}$, $\frac{\partial \mathbf{T}^N}{\partial r_1}$ and $\frac{\partial \mathbf{S}}{\partial r_1}$ are computed from Eqs. (55)-(59). Then the reduced system matrices $\tilde{\mathbf{M}}$, $\tilde{\mathbf{K}}$, $\tilde{\mathbf{C}}$ and $\tilde{\mathbf{f}}$ are calculated by Eqs. (41)-(44). Their derivative matrices $\frac{\partial \tilde{\mathbf{M}}}{\partial r_1}$, $\frac{\partial \tilde{\mathbf{K}}}{\partial r_1}$, $\frac{\partial \tilde{\mathbf{C}}}{\partial r_1}$ and $\frac{\partial \tilde{\mathbf{f}}}{\partial r_1}$ are calculated by Eqs. (51)-(54).

4) The structural responses of the reduced system ($\tilde{\mathbf{x}}$, $\dot{\tilde{\mathbf{x}}}$ and $\ddot{\tilde{\mathbf{x}}}$) and their derivatives ($\frac{\partial \tilde{\mathbf{x}}}{\partial r_1}$, $\frac{\partial \dot{\tilde{\mathbf{x}}}}{\partial r_1}$ and $\frac{\partial \ddot{\tilde{\mathbf{x}}}}{\partial r_1}$) are calculated from Eqs. (40) and (49) respectively, using the Newmark method. In each time step, the Newton Raphson iteration is employed to obtain the accurate time-variant matrices $\tilde{\mathbf{K}}$, $\tilde{\mathbf{C}}$, $\frac{\partial \tilde{\mathbf{K}}}{\partial r_1}$ and $\frac{\partial \tilde{\mathbf{C}}}{\partial r_1}$. The iterations stop when the relative differences of the norm of displacements of all DOFs are less than the predefined tolerance 1×10^{-5}.

5) Finally, the responses and response sensitivities at the nonlinear substructure are extracted directly according to Eqs. (45) and (50), respectively. The responses at the linear substructure are recovered from those of the reduced system by Eqs. (46)-(48). The restrponse sensitivities at the linear substructure are calculated by Eqs. (62)-(64).

In this example, tThe Euclidean norm of $\mathbf{\Phi}_s^L \mathbf{z}_s^L$ in Eq. (33) and its neglectedthe slave inertial item $\mathbf{S}\mathbf{M}^L \mathbf{\Phi}_s^L \ddot{\mathbf{z}}_s^L$ in Eq. (33) are first calculated to investigate the contribution of $\mathbf{SM}^L\boldsymbol{\Phi}_s^L\ddot{\mathbf{z}}_s^L$ to $\boldsymbol{\Phi}_s^L\mathbf{z}_s^L$. In this example, the Euclidean norm of $\mathbf{SM}^L\boldsymbol{\Phi}_s^L\ddot{\mathbf{z}}_s^L$ is as 0.1561 and 3.7894×10^{-15}, – respectivelymuch smaller than $\boldsymbol{\Phi}_s^L\mathbf{z}_s^L$ of 0.1561. The contribution of $\mathbf{SM}^L\boldsymbol{\Phi}_s^L\ddot{\mathbf{z}}_s^L$ is minor and negligibleneglectable.

For comparison, the structural responses are also calculated directly from the global nonlinear vibration equation (Eq. (1)) with the Newmark method and Newton-Raphson iteration method [41]. The response sensitivities are calculated by employing the direct differentiation method to Eq. (1) with an iterative scheme [12]. The process terminates when the displacements of all DOFs converge to the same tolerance 1×10^{-5}. The results are regarded as exact ones.

The displacement response of m_5 by the proposed and global methods are compared in Figure 3. The restoring force of the nonlinear spring is compared in Figure 4. The structural responses and restoring force obtained from the proposed substructuring method are the same as those from the global method, which implies that the proposed method is accurate in computing the structural responses of the nonlinear systems.

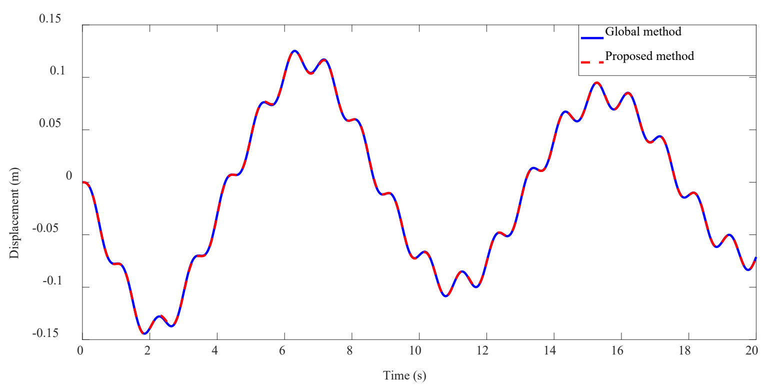

Figure 3. Displacement response of m_5 (x_5).

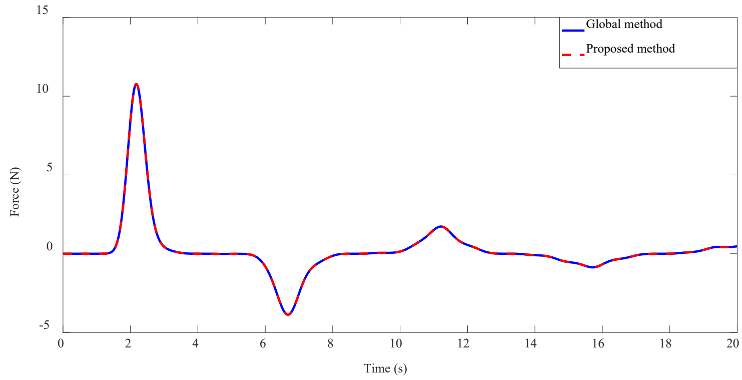

Figure 4. Restoring force of the nonlinear spring (F_s).

To quantify the precision of the proposed method, the relative error of the structural responses is estimated by

$$error\left(\mathbf{X}_S\right)=\frac{\left\|\mathbf{X}_G-\mathbf{X}_S\right\|}{\left\|\mathbf{X}_G\right\|} \tag{66}$$

where $\mathbf{X}_S$ and $\mathbf{X}_G$ respectively denote the structural response or nonlinear restoring force calculated by the proposed substructuring method and the global method and $||\cdot||$ denotes the Euclidean norm of a vector. As shown in Table 1, the relative errors of the responses of all DOFs and the nonlinear restoring force are in the order of 10^{-5} or 10^{-6}. Therefore, the proposed method is very accurate in the calculation of the responses of this nonlinear system.

The response sensitivities are then calculated by the proposed and global methods. Figure 5 compares the derivatives of x_5 and nonlinear restoring force with respect to r_1. Again, the results obtained from the proposed method agree well with those from the global method. The proposed method is also very precise in the calculation of response sensitivities.

Table 1. Relative errors of structural responses and nonlinear restoring force by the proposed method.

Items	$\mathbf{x}$	$\dot{\mathbf{x}}$	$\ddot{\mathbf{x}}$
m_1	2.068×10^{-6}	2.125×10^{-6}	1.245×10^{-6}
m_2	1.368×10^{-6}	2.592×10^{-6}	1.548×10^{-6}
m_3	8.669×10^{-7}	1.692×10^{-6}	1.322×10^{-6}
m_4	1.035×10^{-6}	2.663×10^{-6}	2.894×10^{-6}
m_5	1.073×10^{-6}	2.143×10^{-6}	2.619×10^{-6}
F_s		1.357×10^{-5}	

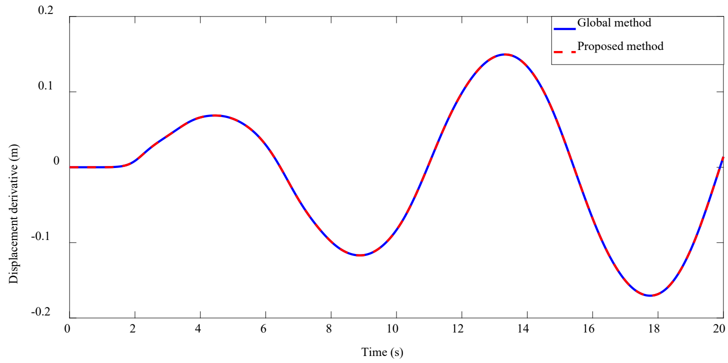

(a) Derivative of x_5 with respect to r_1 ($\frac{\partial x_5}{\partial r_1}$)

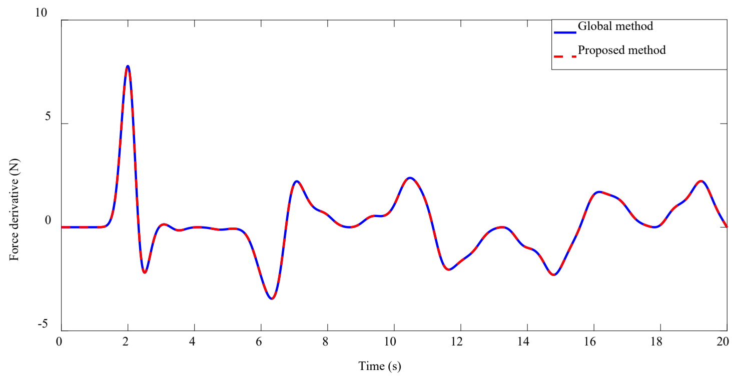

(b) Derivative of F_s with respect to r_1 ($\frac{\partial F_s}{\partial r_1}$)

Figure 5. The response sensitivity with respect to r_1.

Without losing generality, the change ratio of k_s (denoted as r_2 in Figure 1) is also chosen as a design parameter. r_2 is located in the free nonlinear substructure, the independent linear substructural derivative matrices, such as $\frac{\partial \mathbf{K}^L}{\partial r}$, $\frac{\partial \mathbf{M}^L}{\partial r}$, $\frac{\partial \mathbf{F}^L}{\partial r}$, $\frac{\partial \mathbf{\Lambda}_m^L}{\partial r}$, $\frac{\partial \mathbf{\Phi}_m^L}{\partial r}$, $\frac{\partial \mathbf{T}^L}{\partial r}$, $\frac{\partial \mathbf{T}^N}{\partial r}$ and $\frac{\partial \mathbf{S}}{\partial r}$ are therefore zeros as a consequence. The derivatives of the system matrices are obtained directly from Eq. (61). The response sensitivities are then solved directly from Eq. (49) with the Newmark method and Newton-Raphson iteration method. The derivatives of the x_5 and the nonlinear restoring force with respect to r_2 are calculated by the proposed method and are compared with those by the global method in Figure 6. Again, the two curves are almost identical. This indicates that the proposed method is also very accurate to compute the response sensitivities with respect to the nonlinear design parameters.

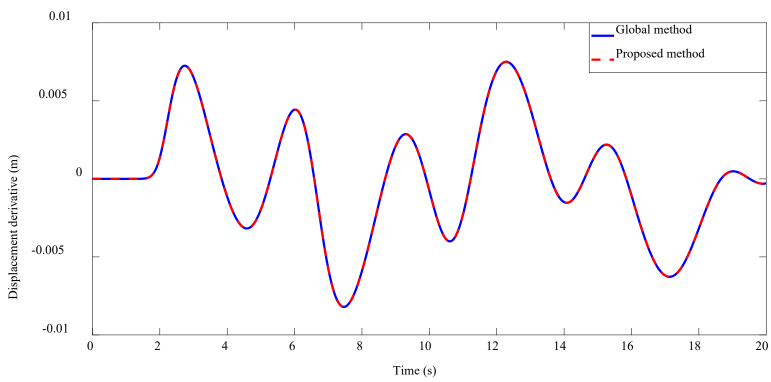

(a) Derivative of x_5 with respect to r_2 ($\frac{\partial x_5}{\partial r_2}$)

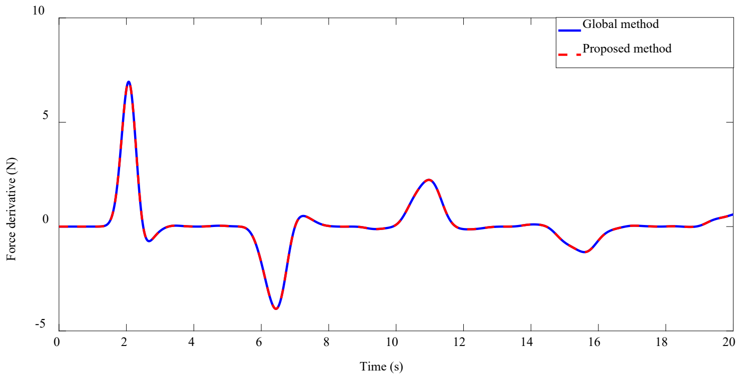

(b) Derivative of F_s with respect to r_2 ($\frac{\partial F_s}{\partial r_2}$)

Figure 6. The response sensitivity with respect to r_2.

Similarly, the relative error of the response sensitivities of the proposed method is quantified by the index

$$error\left(\frac{\partial \mathbf{X}_S}{\partial r}\right) = \frac{\left\| \frac{\partial \mathbf{X}_G}{\partial r} - \frac{\partial \mathbf{X}_S}{\partial r} \right\|}{\left\| \frac{\partial \mathbf{X}_G}{\partial r} \right\|} \tag{67}$$

where $\frac{\partial \mathbf{X}_S}{\partial r}$ and $\frac{\partial \mathbf{X}_G}{\partial r}$ are respectively the response derivative or nonlinear restoring force derivative calculated by the proposed substructuring method and the global method. The relative errors associated with r_1 and r_2 are listed in Table 2. The relative errors of the response and nonlinear restoring force derivatives are in the order of 1×10^{-4} or less. This verifies again that the proposed method is very precise to compute response sensitivities with parameters located in both the linear and nonlinear substructures.

Table 2. Relative errors of responses and nonlinear restoring force derivatives with respect to r_1 and r_2 by the proposed method.

Items	r=r_1			r=r_2		
	$\frac{\partial \mathbf{x}}{\partial r}$	$\frac{\partial \dot{\mathbf{x}}}{\partial r}$	$\frac{\partial \ddot{\mathbf{x}}}{\partial r}$	$\frac{\partial \mathbf{x}}{\partial r}$	$\frac{\partial \dot{\mathbf{x}}}{\partial r}$	$\frac{\partial \ddot{\mathbf{x}}}{\partial r}$
m_1	4.729×10^{-5}	1.040×10^{-4}	7.304×10^{-5}	6.334×10^{-4}	6.424×10^{-4}	6.131×10^{-4}
m_2	3.412×10^{-5}	1.052×10^{-4}	1.650×10^{-4}	6.253×10^{-4}	6.842×10^{-4}	6.693×10^{-4}
m_3	2.300×10^{-5}	8.543×10^{-5}	2.038×10^{-4}	5.707×10^{-4}	7.176×10^{-4}	7.949×10^{-4}
m_4	2.585×10^{-5}	1.154×10^{-4}	1.642×10^{-4}	4.665×10^{-4}	6.740×10^{-4}	3.076×10^{-4}
m_5	3.698×10^{-5}	1.440×10^{-4}	1.741×10^{-4}	5.922×10^{-4}	7.418×10^{-4}	2.594×10^{-4}
$\frac{\partial F_s}{\partial r}$	3.096×10^{-4}			2.609×10^{-4}		

5. Case study 2: a nonlinear frame model

A relatively large frame with a nonlinear viscous damper is then utilized to investigate the accuracy and efficiency of the proposed method. As shown in Figure 7, the frame is modelled with 196 nodes and 216 Euler-Bernoulli beam elements. The model is fixed at Nodes 1, 26, 51 and 76. Each node has 3 in-plane DOFs and the model has 576 DOFs in total. The elemental parameters are as follows: cross-sections of the columns and beams are 800×800 mm^2 and 500×800 mm^2, respectively; Young's modulus is 20 GPa; the mass density is 2500 kg/m^3; and Poisson's ratio is 0.3. The Rayleigh damping is assumed for the structure. The damping coefficients are a_1=1.3255 s^{-1} and a_2=1.3791×10^{-3} s. A nonlinear damper is installed on the structure linking Nodes 1 and 29. The nonlinear force of the damper is [42]

$$f_d = \text{sign}\left(\dot{x}_d\right) C_d \left|\dot{x}_d\right|^{\alpha} \tag{68}$$

where $\dot{x}_d$ is the relative velocity of the two linked nodes along its axial direction, sign(·) is the sign function, C_d is the damping coefficient of the nonlinear damper and α is the exponent of $\dot{x}_d$. In this case, α is set to 0.3 and C_d is 100 kN/(ms^{-1})$^{0.3}$, The frame is excited by the EL Centro earthquake wave in the horizontal direction, which lasts 50 s. The acceleration of the earthquake wave is displayed in Figure 8. The excitation is discretized into 10,000 time steps of 0.005 s. The structural responses and response sensitivities with respect to the change ratio of the damping coefficient C_d (r in Figure 7) will be calculated.

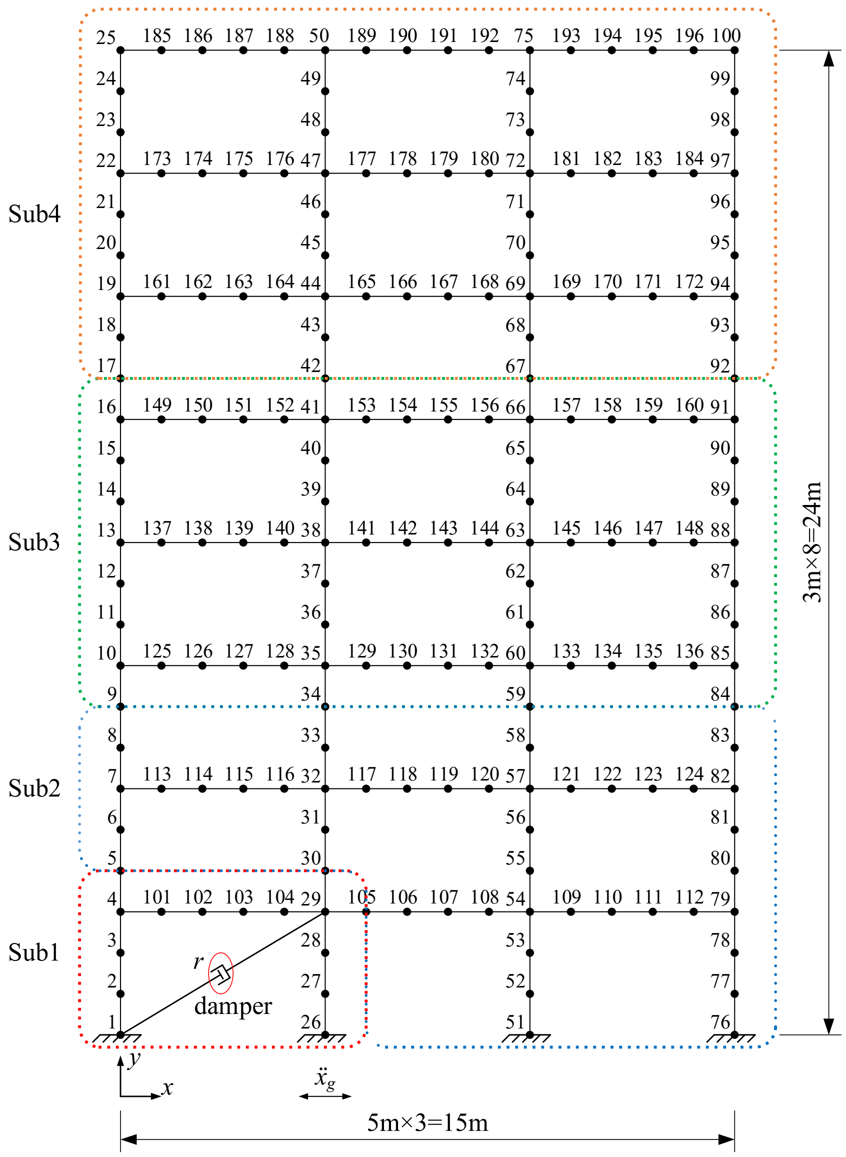

Figure 7. A frame with a nonlinear viscous damper.

The global structure is partitioned into 4 substructures, as shown in Figure 7. The detailed substructural information is listed in Table 3. After partition, the 1st substructure containing the nonlinear viscous damper is treated as a nonlinear substructure, and the other three are linear substructures. The nonlinear substructure has 39 DOFs. The first five modes of each linear substructure are retained as the master modes, and there are 15 master modes in total. In consequence, the system matrices of the reduced vibration equation have the size of 54×54.

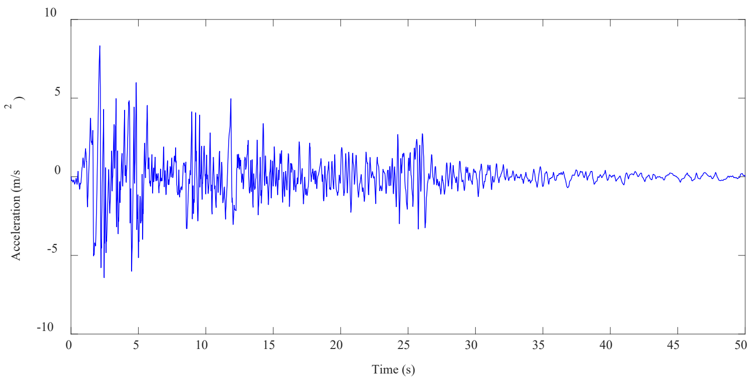

Figure 8. Acceleration of the EL Centro earthquake wave.

Table 3. Substructural information of the frame

Substructures	Sub1	Sub2	Sub3	Sub4
No. nodes	15	48	72	72
No. elements	14	48	77	77
Linear/Nonlinear	Nonlinear	Linear	Linear	Linear
No. Interface nodes	3	4	4	

Again, the structural responses and response sensitivities calculated by the global method are taken as the exact results for comparison. In addition, the modified Craig-Bampton method proposed by Fang et al. [23] is also compared. The method formed the reduced vibration equation with Craig-Bampton's substructuring method. It is a fixed-interface method, and the size of the reduced vibration equation is related to the number of interface DOFs of linear substructures. Identically, the first 5 modes are retained in each linear substructure as master modes, and the reduced system matrices in the modified Craig-Bampton have the size of 78×78. The tolerance of the relative error of the displacement response in the iterative process is set to 1×10^{-5} for all three methods. In each time step, several iterations are required to determine the time-variant reduced system matrices (substructuring methods) or global system matrices (global method). For the entire 10,000 time steps, 38,663, 48,367 and 43,701 iterations are required for the proposed method, Craig-Bampton method and global method, respectively. Fewest iterations are required in the proposed method.

The structural responses are calculated by the three methods. Figure 9 compares the horizontal displacement of a randomly selected node (Node 4) in the nonlinear substructure. A close-up view of the responses is displayed in Figure 9(b). The response curves obtained from the proposed method overlap those from the global method. This implies that the proposed method is accurate to calculate the structural responses of a large nonlinear system with only 5 master modes required in each substructure.

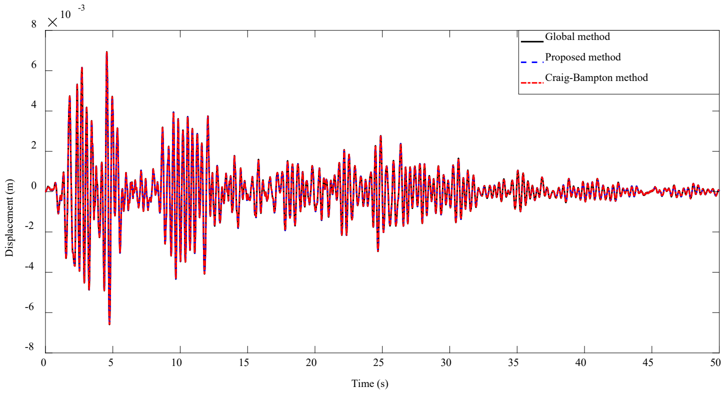

(a) 0-50 s

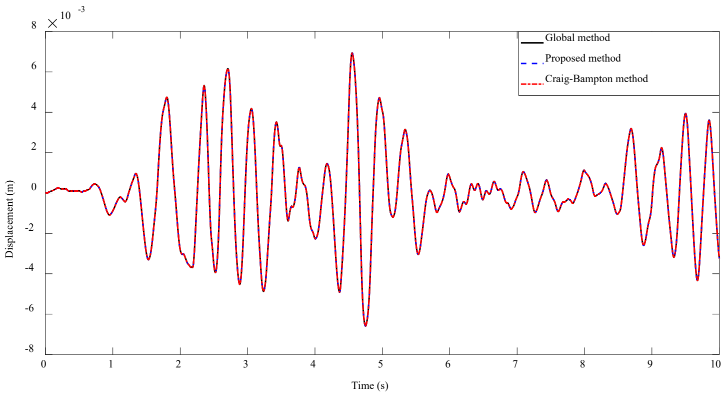

(b) 0-10 s

Figure 9. Horizontal displacement of Node 4 (x_4).

The response sensitivities with respect to r are then calculated by the proposed method. As r is located in the nonlinear substructure, the derivatives of the system matrices are formed directly from Eq. (61), avoiding the computation of many intermediate derivative matrices associated with the linear substructures ($\frac{\partial \mathbf{K}^L}{\partial r}$, $\frac{\partial \mathbf{M}^L}{\partial r}$, $\frac{\partial \mathbf{F}^L}{\partial r}$, $\frac{\partial \mathbf{\Lambda}_m^L}{\partial r}$, $\frac{\partial \mathbf{\Phi}_m^L}{\partial r}$, $\frac{\partial \mathbf{T}^L}{\partial r}$, $\frac{\partial \mathbf{T}^N}{\partial r}$ and $\frac{\partial \mathbf{S}}{\partial r}$). The response sensitivities with respect to r are also calculated by the global method for comparison. Figure 10 compares the derivatives of x_4 with respect to r by the two methods. Again, the results of the proposed method are consistent with those of the global method.

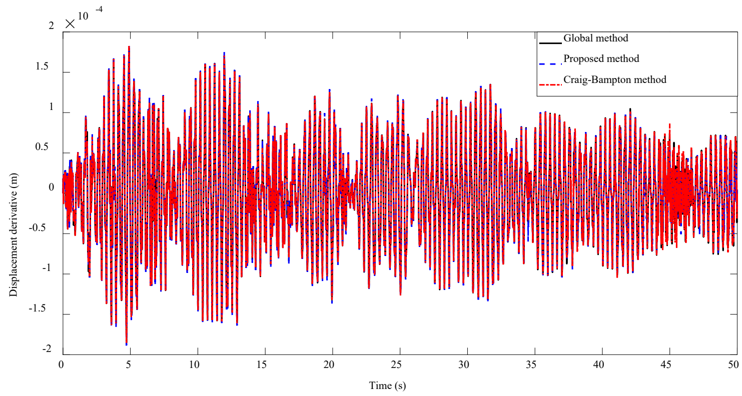

(a) 0-50 s

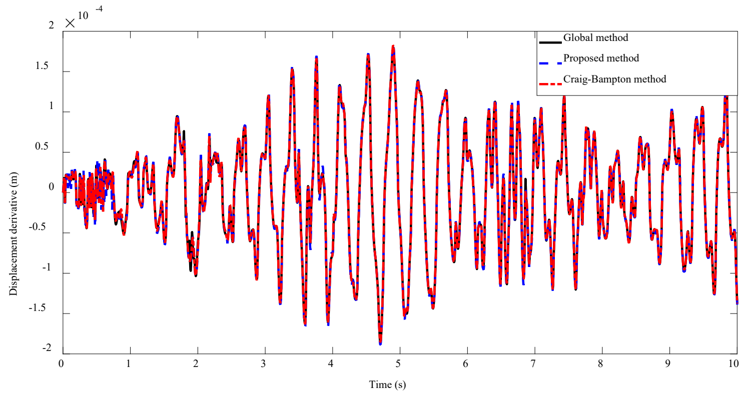

(b) 0-10 s

Figure 10. Derivatives of x_4 with respect to r ($\frac{\partial x_4}{\partial r}$).

To compare the precision of the proposed method and the modified Craig-Bampton method, the relative errors of the methods in structural responses and response sensitivities are estimated by Eqs. (66) and (67), respectively. The results of horizontal displacement responses of all nodes and their derivatives with respect to r are compared in Figures 11 and 12. The relative errors of the proposed method are about the order of 1×10^{-4} for the responses and response sensitivities, smaller than those of the modified Craig-Bampton method. The proposed method is more accurate in the calculation of structural responses and response sensitivities than the modified Craig-Bampton method when the same number of master modes are adopted.

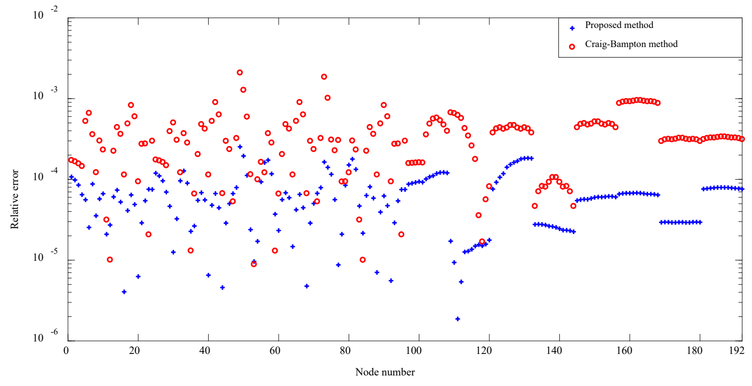

Figure 11. Relative errors of horizontal displacement responses.

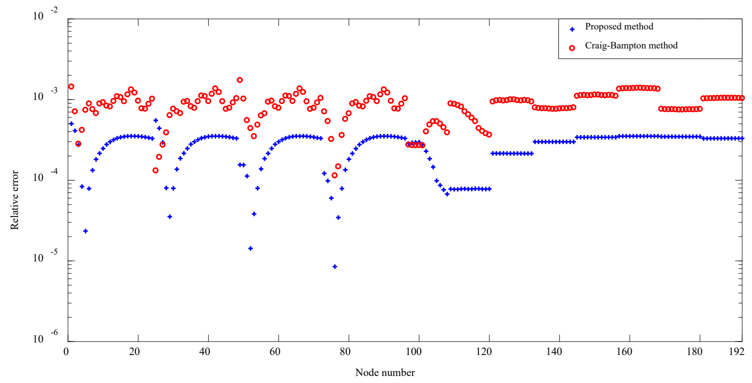

Figure 12. Relative errors of horizontal displacement derivative with respect to *r*.

The CPU time in calculating the structural responses and response sensitivities are compared in Table 4, which runs on the MATLAB platform in a desktop computer with 3.60 GHz CPU and 20 GB RAM. The proposed method takes 0.02 s for the initialization process to form the reduced system vibration equation, and 0.58 s to solve the structural responses with the Newmark method and Newton-Raphson iteration method, totaling 0.60 s for the whole process. In contrast, the traditional global method takes 3.32 s to compute the structural responses. In addition, the proposed method consumes 0.72 s to compute the response sensitivities with respect to one design parameter, while 3.44 s is required for the global method. Therefore, the proposed method is much more efficient than the global method in the calculation of structural responses and response sensitivities. This is because the size of the system matrices of the proposed substructuring method is reduced to 54×54, much smaller than 576×576 in the global method. Although the substructuring method spends a small amount of time in the initialization process, it is negligible compared to the computational time consumed in the Newmark method that takes numerous time steps.

Table 4. Computational time for structural responses and response sensitivities.

Methods	Responses		Response sensitivities		
		Relative ratio	One parameter	All parameters	Relative ratio
Proposed method	0.60 s	18.07%	0.72 s	2.90 min	22.85%
Craig-Bampton method	1.02 s	30.72%	1.18 s	4.32 min	34.04%
Global method	3.32 s	100.00%	3.44 s	12.69 min	100.00%

The modified Craig-Bampton method proposed by Fang et al. [23] is also compared in Table 4. Although the modified Craig-Bampton method can achieve a satisfactory precision as seen in Figures 9-12, it takes 1.02 s and 1.18 s to compute structural responses and response sensitivities, respectively. This is because the reduced vibration equation without interface DOFs has the size of 54×54, smaller than the modified Craig-Bampton method of 78×78. The proposed method neglects the interface DOFs in the reduced vibration equation and is expected to be much more efficient to deal with larger-size nonlinear systems which requires more interface DOFs or complicated interface cases when some specific interface DOFs are shared by three or more substructures.

The precision and efficiency of the substructuring methods are closely related to the number of master modes. To investigate the effects of the number of master modes to the proposed method, the relative error and computational time of the proposed method are estimated with respectivelyusing 9, 15, 24, 36 and 45 master modes considered. The relative errors of x_4 and $\frac{\partial x_4}{\partial r}$ are used as an illustration to estimate the precisioncalculated for different cases, and the results are compared in. Figure 13 compares the precision and efficiency of the proposed method under different numbers of master modes. The computational time consumed for structural responses and response sensitivities is short while the relative errors are large when only 9 master modes are concernedused. With the master modes increasing from 9 to 36, the relative errors drop whereas the computational time increases. As the number of master modes continues to increase, the relative errors only drop slightly while the computational time increase significantly. This implies that the number of master modes is sufficient in this stagecase, inclusion of more master modes has little improvement on the precision. On the contrary, as the number of master modes is comparable to the nonlinear substructural DOFs, inclusion of more master modes enlarges the size of the reduced vibration equation (Eq. (40)) significantly, resulting in low computational efficiency. As a compromise of the computational precision and efficiency, 15 to 36 master modes are suitable for the proposed method according to Figure 13.

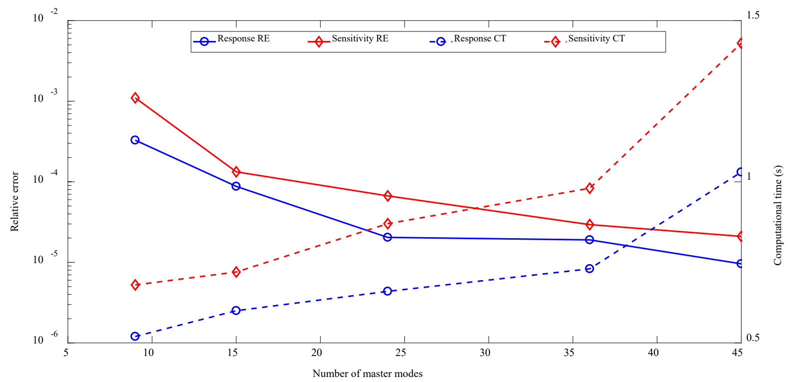

Figure 13. Relative errors (RE) of x_4 and $\frac{\partial x_4}{\partial r}$ and the total computational time (CT) ~~under~~ versus ~~different~~ numbers of master modes.

In model updating or damage detection, the structural model needs to be updated continuously and hundreds of iterations may be required to achieve convergence [32-34]. Within each iteration, the structural responses and response sensitivities with respect to all design parameters have to be calculated. For this example, if C_d and α of the nonlinear damper and the bending rigidities of all elements are selected as the design parameters, there are 218 design parameters in total. The global method takes 12.69 min to compute the response sensitivities with respect to all design parameters, the Craig-Bampton method takes 4.32 min, whereas the proposed substructuring method needs 2.90 min only. If hundreds of iterations are required in model updating or damage detection, the proposed substructuring method can save a lot of computational time. A practical nonlinear system may have thousands of DOFs and design parameters. Calculation of the structural responses and response sensitivities and model updating are very time-consuming. The proposed substructuring method is promising to deal with these cases, which will be studied in the future.

6. Conclusions

This paper develops the Kron's substructuring method to compute the structural responses and response sensitivities of nonlinear systems. The ordinary coherence function is used to detect the presence and location of the nonlinearity. The global structure is then divided into nonlinear and linear substructures. The size of the linear substructures is reduced to a small size of master modes after a simplified processwith compensation of the slave modes, and the expensive nonlinear analysis is only constrained in the local area other than the global structure. Since the linear parts are reduced and the nonlinear analysis is localized at the substructure level, the proposed substructuring method can significantly improve the computation efficiency. Applications to a nonlinear spring-mass system and a nonlinear frame show that the proposed method is accurate and efficient to compute the structural responses and response sensitivities of nonlinear systems.

Acknowledgements

The work described in this paper is supported by the National Natural Science Foundation of China (NSFC, contract number: 51778258 and 51922046) and the National Key R&D Program (Project No. 2019YFB1600702).

References

[1] K. Worden, G.R. Tomlinson, Nonlinearity in structural dynamics: detection, identification and modelling, Institute of Physics Publishing, 2001.

[2] G. Kerschen, K. Worden, A.F. Vakakis, J.C. Golinval, Past, present and future of nonlinear system identification in structural dynamics, Mech. Syst. Signal Process. 20 (3) (2006) 505-592.

[3] Z.R. Lu, R.Z. Yao, L. Wang, J.K. Liu, Identification of nonlinear hysteretic parameters by enhanced response sensitivity approach, Int. J. Nonlin. Mech. 96 (2017) 1-11.

[4] J.W. Zhan, H. Xia, S.Y. Chen, G. de Roeck, Structural damage identification for railway bridges based on train-induced bridge responses and sensitivity analysis, J. Sound Vib. 330 (4) (2011) 757-770.

[5] Z.R. Lu, L. Wang, An enhanced response sensitivity approach for structural damage identification: convergence and performance, Int. J. Numer. Meth. Eng. 111 (13) (2017) 1231-1251.

[6] R.E. Melchers, M. Ahammed, A fast approximate method for parameter sensitivity estimation in Monte Carlo structural reliability, Comput. Struct. 82 (1) (2004) 55-61.

[7] N. Pollini, O. Lavan, O. Amir, Adjoint sensitivity analysis and optimization of hysteretic dynamic systems with nonlinear viscous dampers, Struct. Multidiscip. O. 57 (6) (2018) 2273-2289.

[8] H.S. Gopalakrishna, L.F. Greimann, Newton-Raphson procedure for the sensitivity analysis of nonlinear structural behavior, Comput. Struct. 30 (6) (1988) 1263-1273.

[9] C. Grossmann, H.G. Roos, M. Stynes, Numerical treatment of partial differential equations, *Springer*, 2007.

[10] R. Kiran, L. Li, K. Khandelwal, Complex perturbation method for sensitivity analysis of nonlinear trusses, J. Struct. Eng. 143 (1) (2017) 04016154.

[11] W.J. Wang, P.M. Clausen, K.U. Bletzinger, Efficient adjoint sensitivity analysis of isotropic hardening elastoplasticity via load steps reduction approximation, Comput. Method. Appl. M. 325 (2017) 612-644.

[12] Q. Gu, L. Wang, Y. Li, X. Deng, C. Lin, Multi-scale response sensitivity analysis based on direct differentiation method for concrete structures, Compos. Part B-Eng. 157 (2019) 295-304.

[13] D. de Klerk, D.J. Rixen, S.N. Voormeeren, General framework for dynamic substructuring: history, review, and classification of techniques, AIAA J. 46 (5) (2008) 1169-1181.

[14] S. Weng, H.P. Zhu, Y. Xia, J.J. Li, W. Tian, A review on dynamic substructuring methods for model updating and damage detection of large-scale structures, Adv. Struct. Eng. 23 (3) (2020) 584-600.

[15] W.C. Hurty, Vibrations of structural systems by component mode synthesis, J. Eng. Mech. Div. 86 (4) (1960) 51-69.

[16] R.R. Craig, M.C.C. Bampton, Coupling of substructures for dynamic analyses, AIAA J. 6 (7) (1968) 1313-1319.

[17] Z.Q. Qu, Model reduction for dynamical systems with local nonlinearities, AIAA J. 40 (2) (2002) 327:333.

[18] P. Apiwattanalunggarn, S.W. Shaw, C. Pierre, Component mode synthesis using nonlinear normal modes, Nonlinear Dynam. 41 (1-3) (2005) 17-46.

[19] D. Jiang, C. Pierre, S.W. Shaw, The construction of nonlinear normal modes for systems with internal resonance, Int. J. Nonlin. Mech. 40 (5) (2005) 729-746.

[20] G. Kerschen, M. Peeters, J.C. Golinval, A.F. Vakakis, Nonlinear normal modes, Part I: A useful framework for the structural dynamicist, Mech. Syst. Signal Pr. 23 (1) (2009) 170-194.

[21] G. Kerschen, M. Peeters, J.C. Golinval, C. Stephan, Nonlinear modal analysis of a full-scale aircraft, J. Aircraft. 50 (5) (2013) 1409-1419.

[22] C. Joannin, B. Chouvion, F. Thouverez, J.P. Ousty, M. Mbaye, A nonlinear component mode synthesis method for the computation of steady-state vibrations

in non-conservative systems, Mech. Syst. Signal Pr. 83 (2017) 75-92.

[23] M. Fang, J. Wang, H. Li, An adaptive numerical scheme based on the Craig-Bampton method for the dynamic analysis of tall buildings, Struct. Des. Tall Spec. 27 (2018) e1410.

[24] F. Latini, J. Brunetti, W. D'Ambrogio, A. Fregolent, Substructures' coupling with nonlinear connecting elements, Nonlinear Dynam. 99 (2020) 1643-1658.

[25] G. Kron, Diakoptics, Macdonald and Co., London, 1963.

[26] A. Simpson, B. Tabarrok, On Kron's eigenvalue procedure and related methods of frequency analysis, Q. J. Mech. Appl. Math. 21 (1) (1968) 1-39.

[27] A. Simpson, Eigenvalue and vector sensitivities in Kron's method, J. Sound Vib. 31 (1) (1973) 73-87.

[28] S. Weng, Y. Xia, Y.L. Xu, X.Q. Zhou, H.P. Zhu, Improved substructuring method for eigensolutions of large-scale structures, J. Sound Vib. 323 (3-5) (2009) 718-736.

[29] Y. Xia, S. Weng, Y.L. Xu, H.P. Zhu, (2010), Calculation of eigenvalue and eigenvector derivatives with the improved Kron's substructuring method, Struct. Eng. Mech. 36 (1) (2010) 37-55.

[30] J. Cui, X. Guan, G.T. Zheng, A simultaneous iterative procedure for the Kron's component modal synthesis approach, Int. J. Numer. Meth. Eng. 105 (13) (2016) 990-1013.

[31] W. Tian, S. Weng, Y. Xia, H.P. Zhu, F. Gao, Y. Sun, J.J. Li, An iterative reduced-order substructuring approach to the calculation of eigensolutions and eigensensitivities, Mech. Syst. Signal Pr. 130 (2019) 361-377.

[32] S. Weng, Y. Xia, X.Q. Zhou, Y.L. Xu, H.P. Zhu, Inverse substructure method for model updating of structures, J. Sound Vib. 331 (25) (2012) 5449-5468.

[33] H.P. Zhu, J.J. Li, W. Tian, S. Weng, Y.C. Peng, Z.X. Zhang, Z.D. Chen, An enhanced substructure-based response sensitivity method for finite element model updating of large-scale structures, Mech. Syst. Signal Pr. 154 (2021) 107359.

[34] S. Weng, H.P. Zhu, Y. Xia, L. Mao, Damage detection using the eigenparameter decomposition of substructural flexibility matrix, Mech. Syst. Signal Pr. 34 (1-2) (2013) 19-38.

[35] Y. Li, S.R. Huang, C. Lin, Q. Gu, Z.J. Qiu, Response sensitivity analysis for plastic plane problems based on direct differentiation method, Comput Struct. 182 (2017) 392-403.

[36] L.C. Rogers, Derivatives of eigenvalues and eigenvectors, AIAA J. 8 (5) (1970) 943-944.

[37] R.B. Nelson, Simplified calculation of eigenvector derivatives, AIAA J. 14 (9) (1976) 1201-1205.

[38] J.P. Noel, G. Kerschen, Nonlinear system identification in structural dynamics: 10 more years of progress, Mech. Syst. Signal Pr. 83 (2017) 2-35.

[39] D.E. Newland, An introduction to random vibrations, spectral and wavelet analysis, Prentice-Hall, Harlow, 1993.

[40] R.J. Allemang, D.L. Brown, Experimental modal analysis and dynamic component analysis−vol. 2: measurement techniques for experimental modal analysis, AFWAL Technical Report TR 87-3069, 1987.

[41] F.F. Taucer, E. Spacone, F.C. Filippou. A fiber beam-column element for seismic response analysis of reinforced concrete structures, California: Earthquake Engineering Research Center, College of Engineering, University of California Berkekey, 1991.

[42] F. Li, S. Zhang, H.J. Peng, B.S. Chen, The model predictive control for structural vibration with local nonlinearity, Chin. J. Comput. Mech. 35 (5) (2018) 582-588 (in Chinese).